immuno-dominant $CD8^+$ T-cell epitope.[52] Therefore, there is a limitation to our study, because the number of immunogenic AFP-derived peptides applicable in this study is small. However, the results of the present study suggest that TAE with DC infusion enhances the tumor-specific immune responses. Although these modified immune responses may not be sufficient to prevent HCC recurrence because the enhanced immune responses are transient and attenuate within 3 months, these results may contribute to the development of novel immunotherapeutic approach for HCC.

Acknowledgements

The authors thank Ms. Maki Kawamura and Ms. Kazumi Fushimi for technical assistance and for their invaluable help with sample collection.

References

1. Curley SA, Izzo F, Ellis LM, Nicolas Vauthey J, Vallone P. Radiofrequency ablation of hepatocellular cancer in 110 patients with cirrhosis. *Ann Surg* 2000;232: 381–91.
2. Mazzaferro V, Regalia E, Doci R, Andreola S, Pulvirenti A, Bozzetti F, Montalto F, Ammatuna M, Morabito A, Gennari L. Liver transplantation for the treatment of small hepatocellular carcinomas in patients with cirrhosis. *N Engl J Med* 1996;334: 693–9.
3. Urabe T, Kaneko S, Matsushita E, Unoura M, Kobayashi K. Clinical pilot study of intrahepatic arterial chemotherapy with methotrexate, 5-fluorouracil, cisplatin and subcutaneous interferon-alpha-2b for patients with locally advanced hepatocellular carcinoma. *Oncology* 1998; 55:39–47.
4. Ishizaki Y, Kawasaki S. The evolution of liver transplantation for hepatocellular carcinoma (past, present, and future). *J Gastroenterol* 2008;43:18–26.
5. Okuwaki Y, Nakazawa T, Shibuya A, Ono K, Hidaka H, Watanabe M, Kokubu S, Saigenji K. Intrahepatic distant recurrence after radiofrequency ablation for a single small hepatocellular carcinoma: risk factors and patterns. *J Gastroenterol* 2008;43:71–8.
6. Abdel-Hady ES, Martin-Hirsch P, Duggan-Keen M, Stern PL, Moore JV, Corbitt G, Kitchener HC, Hampson IN. Immunological and viral factors associated with the response of vulval intraepithelial neoplasia to photodynamic therapy. *Cancer Res* 2001;61:192–6.
7. Nakamoto Y, Mizukoshi E, Tsuji H, Sakai Y, Kitahara M, Arai K, Yamashita T, Yokoyama K, Mukaida N, Matsushima K, Matsui O, Kaneko S. Combined therapy of transcatheter hepatic arterial embolization with intratumoral dendritic cell infusion for hepatocellular carcinoma: clinical safety. *Clin Exp Immunol* 2007;147: 296–305.
8. Ayaru L, Pereira SP, Alisa A, Pathan AA, Williams R, Davidson B, Burroughs AK, Meyer T, Behboudi S. Unmasking of alpha-fetoprotein-specific CD4(+) T cell responses in hepatocellular carcinoma patients undergoing embolization. *J Immunol* 2007;178:1914–22.
9. Zerbini A, Pilli M, Penna A, Pelosi G, Schianchi C, Molinari A, Schivazappa S, Zibera C, Fagnoni FF, Ferrari C, Missale G. Radiofrequency thermal ablation of hepatocellular carcinoma liver nodules can activate and enhance tumor-specific T-cell responses. *Cancer Res* 2006;66:1139–46.
10. Mizukoshi E, Nakamoto Y, Tsuji H, Yamashita T, Kaneko S. Identification of alpha-fetoprotein-derived peptides recognized by cytotoxic T lymphocytes in HLA-A24+ patients with hepatocellular carcinoma. *Int J Cancer* 2006;118: 1194–204.
11. Gollnick SO, Evans SS, Baumann H, Owczarczak B, Maier P, Vaughan L, Wang WC, Unger E, Henderson BW. Role of cytokines in photodynamic therapy-induced local and systemic inflammation. *Br J Cancer* 2003;88:1772–9.
12. Gollnick SO, Owczarczak B, Maier P. Photodynamic therapy and anti-tumor immunity. *Lasers Surg Med* 2006;38: 509–15.
13. Yamamoto N, Homma S, Sery TW, Donoso LA, Hoober JK. Photodynamic immunopotentiation: in vitro activation of macrophages by treatment of mouse peritoneal cells with haematoporphyrin derivative and light. *Eur J Cancer* 1991;27: 467–71.
14. den Brok MH, Sutmuller RP, van der Voort R, Bennink EJ, Figdor CG, Ruers TJ, Adema GJ. In situ tumor ablation creates an antigen source for the generation of antitumor immunity. *Cancer Res* 2004;64: 4024–9.
15. Kotera Y, Shimizu K, Mule JJ. Comparative analysis of necrotic and apoptotic tumor cells as a source of antigen(s) in dendritic cell-based immunization. *Cancer Res* 2001; 61:8105–9.
16. Sauter B, Albert ML, Francisco L, Larsson M, Somersan S, Bhardwaj N. Consequences of cell death: exposure to necrotic tumor cells, but not primary tissue cells or apoptotic cells, induces the maturation of immunostimulatory dendritic cells. *J Exp Med* 2000;191:423–34.
17. Korbelik M, Sun J, Cecic I. Photodynamic therapy-induced cell surface expression and release of heat shock proteins: relevance for tumor response. *Cancer Res* 2005;65: 1018–26.
18. Takayasu K, Arii S, Ikai I, Omata M, Okita K, Ichida T, Matsuyama Y, Nakanuma Y, Kojiro M, Makuuchi M, Yamaoka Y. Prospective cohort study of transarterial chemoembolization for unresectable hepatocellular carcinoma in 8510 patients. *Gastroenterology* 2006;131:461–9.
19. Matsui O, Kadoya M, Yoshikawa J, Gabata T, Arai K, Demachi H, Miyayama S, Takashima T, Unoura M, Kogayashi K. Small hepatocellular carcinoma: treatment with subsegmental transcatheter arterial embolization. *Radiology* 1993;188:79–83.
20. Yamada R, Kishi K, Sonomura T, Tsuda M, Nomura S, Satoh M. Transcatheter arterial embolization in unresectable hepatocellular carcinoma. *Cardiovasc Intervent Radiol* 1990;13:135–9.
21. Pelletier G, Roche A, Ink O, Anciaux ML, Derhy S, Rougier P, Lenoir C, Attali P, Etienne JP. A randomized trial of hepatic arterial chemoembolization in patients with unresectable hepatocellular carcinoma. *J Hepatol* 1990;11:181–4.
22. Groupe d'Etude et de Traitement du Carcinome Hepatocellulaire. A comparison of lipiodol chemoembolization and conservative treatment for unresectable hepatocellular carcinoma. *N Engl J Med* 1995;332:1256–61.
23. Bruix J, Llovet JM, Castells A, Montana X, Bru C, Ayuso MC, Vilana R, Rodes J. Transarterial embolization versus symptomatic treatment in patients with advanced hepatocellular carcinoma: results of a randomized, controlled trial in a single institution. *Hepatology* 1998;27:1578–83.
24. Llovet JM, Real MI, Montana X, Planas R, Coll S, Aponte J, Ayuso C, Sala M, Muchart J, Sola R, Rodes J, Bruix J. Arterial embolisation or chemoembolisation versus symptomatic treatment in patients with unresectable hepatocellular carcinoma: a randomised controlled trial. *Lancet* 2002;359:1734–9.
25. Lo CM, Ngan H, Tso WK, Liu CL, Lam CM, Poon RT, Fan ST, Wong J. Randomized controlled trial of transarterial lipiodol chemoembolization for unresectable hepatocellular carcinoma. *Hepatology* 2002;35:1164–71.
26. Hsu HC, Wei TC, Tsang YM, Wu MZ, Lin YH, Chuang SM. Histologic assessment of resected hepatocellular carcinoma after

transcatheter hepatic arterial embolization. *Cancer* 1986;57:1184–91.
27. Kenji J, Hyodo I, Tanimizu M, Tanada M, Nishikawa Y, Hosokawa Y, Mandai K, Moriwaki S. Total necrosis of hepatocellular carcinoma with a combination therapy of arterial infusion of chemotherapeutic lipiodol and transcatheter arterial embolization: report of 14 cases. *Semin Oncol* 1997;24: S6-71–S6-80.
28. Kobayashi N, Ishii M, Ueno Y, Kisara N, Chida N, Iwasaki T, Toyota T. Co-expression of Bcl-2 protein and vascular endothelial growth factor in hepatocellular carcinomas treated by chemoembolization. *Liver* 1999;19:25–31.
29. Xiao EH, Li JQ, Huang JF. Effects of p53 on apoptosis and proliferation of hepatocellular carcinoma cells treated with transcatheter arterial chemoembolization. *World J Gastroenterol* 2004;10:190–4.
30. Kanai M, Kohda H, Sekiya C, Namiki M. Effects on interleukin 1 alpha and beta production of peripheral blood mononuclear cells from patients with hepatocellular carcinoma after transcatheter arterial embolization. *Gastroenterol Jpn* 1990;25:662.
31. Yamazaki H, Nishimoto N, Oi H, Matsushita M, Ogata A, Shima Y, Inoue T, Tang JT, Yoshizaki K, Kishimoto T, Inoue T. Serum interleukin 6 as a predicator of the therapeutic effect and adverse reactions after transcatheter arterial embolization. *Cytokine* 1995;7:191–5.
32. Itoh Y, Okanoue T, Ohnishi N, Nishioji K, Sakamoto S, Nagao Y, Nakamura H, Kirishima T, Kashima K. Hepatic damage induced by transcatheter arterial chemoembolization elevates serum concentrations of macrophage-colony stimulating factor. *Liver* 1999;19:97–103.
33. Araki T, Itai Y, Furui S, Tasaka A. Dynamic CT densitometry of hepatic tumors. *AJR Am J Roentgenol* 1980;135: 1037–43.
34. Sobin LH, Wittekind C. TNM classification of malignant tumors, 6th edn. New York: Wiley-Liss, 2002. 81.
35. Terayama N, Miyayama S, Tatsu H, Yamamoto T, Toya D, Tanaka N, Mitsui T, Miura S, Fujisawa M, Kifune K, Matsui O, Takashima T. Subsegmental transcatheter arterial embolization for hepatocellular carcinoma in the caudate lobe. *J Vasc Interv Radiol* 1998;9:501–8.
36. Okamoto H, Shin J, Mion S, Koshimura S, Shimizu R. Studies on the anticancer and streptolysin S-forming abilities of hemolytic streptococci. *Jpn J Microbiol* 1967;11: 323–36.
37. Nakahara S, Tsunoda T, Baba T, Asabe S, Tahara H. Dendritic cells stimulated with a bacterial product, OK-432, efficiently induce cytotoxic T lymphocytes specific to tumor rejection peptide. *Cancer Res* 2003; 63:4112–8.
38. Japan LCSGo. Classification of primary liver cancer. English edn. 2. Tokyo: Kanehara, 1997.
39. Desmet VJ, Gerber M, Hoofnagle JH, Manns M, Scheuer PJ. Classification of chronic hepatitis: diagnosis, grading and staging. *Hepatology* 1994;19:1513–20.
40. Mizukoshi E, Nakamoto Y, Marukawa Y, Arai K, Yamashita T, Tsuji H, Kuzushima K, Takiguchi M, Kaneko S. Cytotoxic T cell responses to human telomerase reverse transcriptase in patients with hepatocellular carcinoma. *Hepatology* 2006;43:1284–94.
41. Mizukoshi E, Honda M, Arai K, Yamashita T, Nakamoto Y, Kaneko S. Expression of multidrug resistance-associated protein 3 and cytotoxic T cell responses in patients with hepatocellular carcinoma. *J Hepatol* 2008;49:946–54.
42. Ikeda-Moore Y, Tomiyama H, Miwa K, Oka S, Iwamoto A, Kaneko Y, Takiguchi M. Identification and characterization of multiple HLA-A24-restricted HIV-1 CTL epitopes: strong epitopes are derived from V regions of HIV-1. *J Immunol* 1997;159: 6242–52.
43. Kuzushima K, Hayashi N, Kimura H, Tsurumi T. Efficient identification of HLA-A*2402-restricted cytomegalovirus-specific CD8(+) T-cell epitopes by a computer algorithm and an enzyme-linked immunospot assay. *Blood* 2001;98:1872–81.
44. Wissniowski TT, Hansler J, Neureiter D, Frieser M, Schaber S, Esslinger B, Voll R, Strobel D, Hahn EG, Schuppan D. Activation of tumor-specific T lymphocytes by radio-frequency ablation of the VX2 hepatoma in rabbits. *Cancer Res* 2003;63: 6496–500.
45. Korbelik M, Krosl G, Krosl J, Dougherty GJ. The role of host lymphoid populations in the response of mouse EMT6 tumor to photodynamic therapy. *Cancer Res* 1996;56: 5647–52.
46. Udagawa M, Kudo-Saito C, Hasegawa G, Yano K, Yamamoto A, Yaguchi M, Toda M, Azuma I, Iwai T, Kawakami Y. Enhancement of immunologic tumor regression by intratumoral administration of dendritic cells in combination with cryoablative tumor pretreatment and Bacillus Calmette-Guerin cell wall skeleton stimulation. *Clin Cancer Res* 2006;12: 7465–75.
47. Machlenkin A, Goldberger O, Tirosh B, Paz A, Volovitz I, Bar-Haim E, Lee SH, Vadai E, Tzehoval E, Eisenbach L. Combined dendritic cell cryotherapy of tumor induces systemic antimetastatic immunity. *Clin Cancer Res* 2005;11: 4955–61.
48. Ladhams A, Schmidt C, Sing G, Butterworth L, Fielding G, Tesar P, Strong R, Leggett B, Powell L, Maddern G, Ellem K, Cooksley G. Treatment of non-resectable hepatocellular carcinoma with autologous tumor-pulsed dendritic cells. *J Gastroenterol Hepatol* 2002;17: 889–96.
49. Iwashita Y, Tahara K, Goto S, Sasaki A, Kai S, Seike M, Chen CL, Kawano K, Kitano S. A phase I study of autologous dendritic cell-based immunotherapy for patients with unresectable primary liver cancer. *Cancer Immunol Immunother* 2003; 52:155–61.
50. Lee WC, Wang HC, Hung CF, Huang PF, Lia CR, Chen MF. Vaccination of advanced hepatocellular carcinoma patients with tumor lysate-pulsed dendritic cells: a clinical trial. *J Immunother* 2005;28: 496–504.
51. Lee JS, Thorgeirsson SS. Genome-scale profiling of gene expression in hepatocellular carcinoma: classification, survival prediction, and identification of therapeutic targets. *Gastroenterology* 2004; 127:S51–5.
52. Thimme R, Neagu M, Boettler T, Neumann-Haefelin C, Kersting N, Geissler M, Makowiec F, Obermaier R, Hopt UT, Blum HE, Spangenberg HC. Comprehensive analysis of the alpha-fetoprotein-specific CD8+ T cell responses in patients with hepatocellular carcinoma. *Hepatology* 2008;48:1821–33.

Clin Orthop Relat Res (2010) 468:1373–1383
DOI 10.1007/s11999-010-1302-z

BASIC RESEARCH

Cryoimmunologic Antitumor Effects Enhanced by Dendritic Cells in Osteosarcoma

Masanori Kawano MD, Hideji Nishida MD, PhD, Yasunari Nakamoto MD, PhD, Hiroshi Tsumura MD, PhD, Hiroyuki Tsuchiya MD, PhD

Received: 20 February 2009 / Accepted: 1 March 2010 / Published online: 16 March 2010

Abstract

Background We previously reported a limb-salvage technique by treating tumor-bearing bone with liquid nitrogen. We also reported systemic antitumor immunity was enhanced by cryotreatment in a murine osteosarcoma (LM8) model. We therefore combined the cryotreatment of tumor with dendritic cells to promote tumor-specific immune responses.

Questions/purposes We determined whether our technique could enhance systemic immune response and inhibit metastatic tumor growth in a murine osteosarcoma model.

Materials and Methods To evaluate activation of the immune response, we prepared six groups of C3H mice (80 mice total): (1) excision only, (2) dendritic cells without reimplantation of the cryotreated primary tumor, (3) reimplantation of the cryotreated primary tumor alone, (4) dendritic cells combined with reimplantation of the cryotreated primary tumor, (5) dendritic cells exposed to cryotreated tumor lysates without reimplantation of the cryotreated primary tumor, and (6) dendritic cells exposed to cryotreated tumor lysates with reimplantation of the cryotreated primary tumor. We then compared and verified the activation state of each group's antitumor immunity.

Results Mice that received dendritic cells exposed to cryotreated tumor lysates with reimplantation of the cryotreated primary tumor group had high serum interferon γ, reduced pulmonary metastases, and increased numbers of CD8(+) T lymphocytes in the metastatic areas.

Conclusions Combining tumor cryotreatment with dendritic cells enhanced systemic immune responses and inhibited metastatic tumor growth.

Clinical Relevance We suggest immunotherapy could be developed further to improve the treatment of osteosarcoma.

Introduction

The standard treatment of osteosarcoma consists of preoperative chemotherapy, surgical tumor excision, and postoperative chemotherapy. Limb-saving surgery is feasible in most cases. Advances in osteosarcoma treatment have now achieved a 5-year survival rate of 60% to 90% for patients, and limb function after reconstruction continues to improve with time [3, 16, 30, 46, 47, 49].

Tsuchiya et al. developed a new approach using frozen autografts [48] to improve reconstruction after osteosarcoma resection. The tumor is resected with an adequate margin, and the resected specimen is immersed in liquid

Each author certifies that he or she has no commercial associations that might pose a conflict of interest in connection with the submitted article.
Each author certifies that his or her institution has approved the animal protocol for this investigation, and that all investigations were conducted in conformity with ethical principles of research.
This work was performed at the Department of Orthopaedic Surgery, Graduate School of Medical Science, Kanazawa University, and the Department of Orthopaedic Surgery, Faculty of Medicine, Oita University.

M. Kawano, H. Nishida, H. Tsuchiya (✉)
Department of Orthopaedic Surgery, Graduate School of Medical Science, Kanazawa University, 13-1 Takara-machi, Kanazawa 920-8641, Japan
e-mail: tsuchi@med.kanazawa-u.ac.jp

M. Kawano, H. Tsumura
Department of Orthopaedics Surgery, Faculty of Medicine, Oita University, Oita, Japan

Y. Nakamoto
Department of Gastroenterology, Graduate School of Medical Science, Kanazawa University, Kanazawa, Japan

nitrogen for 20 minutes to kill all tumor cells. After thawing, the specimen is returned to the original place with appropriate internal fixation to reconstruct the defect. Compared with heat-treated bones [8, 14], bone genetic proteins and native biomechanical structures are preserved after cryotreatment [53]. In one report limb function using the technique of Tsuchiya et al. was rated as excellent in 71.4% of patients, and good in 10.7%, as assessed by the functional evaluation system of Enneking [11]. Two studies suggest the approach enhanced bone formation when compared histologically with pasteurized bone and irradiated bone [43, 48]. Another advantage in reimplanting cryotreated tumor tissue is its effect on the immune system [50]: tumor tissue after cryoablation in situ provokes an immune reaction in patients with breast and prostate cancer [6, 8, 39]. Brewer et al. reported metastatic tumors sometimes disappear or shrink after in situ cryoablation of the primary tumor with liquid nitrogen [4]. The structure of tumor antigens is retained in frozen tumor, and leukocytes probably can recognize these antigens. Similar antitumor effects can be expected from our reconstructive procedure of reimplanting tumor-bearing bone after cryotreatment with liquid nitrogen.

Nishida et al. observed an inadequate antitumor effect after reimplantation of frozen tumor tissue alone [35]. However, the antitumor effect was enhanced by promoting nonspecific immune activation by intraperitoneal injection of OK-432, a substance extracted from alpha-Streptococcus pyogenes. This approach promotes inflammation and activation of dendritic cells (DCs) that initiate the specific antitumor effect [19]. This type of immunotherapy reportedly is effective for breast and prostate cancers [6, 8, 39]. Many groups have reported successful immunotherapy for osteosarcoma [5, 15, 18, 20, 22, 24, 25, 33, 34, 36, 42, 51, 52]. However, the ability to control metastatic lesions and local recurrence does not appear to be superior to other adjuvant treatments [2, 7, 13, 23, 29].

We therefore wondered whether combining cryotreatment and immunotherapy might enhance tumor response. We specifically determined whether: (1) antitumor immunity could be enhanced through activation and transfer of DCs combined with reimplantation of the cryotreated primary tumor, and (2) metastatic lesions could be prevented owing to the involvement of T lymphocytes in a murine osteosarcoma model (LM8).

Materials and Methods

Using a reported method to induce osteosarcoma [1, 35], we hypodermically implanted 1×10^6 LM8 cells (a murine osteosarcoma cell line) into the subcutaneous gluteal region of 80 female C3H mice, 6 to 8 weeks old. Tumors developed in all animals. Two weeks after inoculation, we surgically excised the tumors and cryotreated them with liquid nitrogen. We established the following six groups (Fig. 1): (1) the tumor was excised with wide margins 14 days after inoculation (n = 15); (2) the tumor was excised with wide margins 14 days after inoculation and bone marrow-derived DCs then were injected into the contralateral subcutaneous gluteal region without reimplantation of the cryotreated primary tumor twice a week (n = 15); (3) the tumor was excised with wide margins 14 days after inoculation and reimplanted after cryotreatment with liquid nitrogen into the contralateral gluteal region to evaluate for local recurrence from frozen tumor tissue (n = 15); (4) the tumor was excised 14 days after inoculation and reimplanted after cryotreatment into the contralateral gluteal region to evaluate for local recurrence, and DCs then were injected twice a week into this secondary site (n = 15); (5) the tumor was excised with wide margins 14 days after inoculation and DCs exposed to cryotreated tumor lysates were injected twice a week into the contralateral gluteal region without reimplantation of the cryotreated primary tumor (n = 15); and (6) the tumor was excised with wide margins 14 days after inoculation and reimplanted after the treatment with liquid nitrogen into the contralateral gluteal region to evaluate for local recurrence (same as Group 3) with the addition of DCs exposed to cryotreated tumor lysates injected twice a week (n = 15). We harvested tumor from 30 mice, and then the tumor was treated with liquid nitrogen to create the lysates. We presumed a systemic immune response would be induced by injecting DCs around the frozen tumor tissue. We microscopically determined the presence of metastases in the lungs 2 weeks after the tumor inoculation. We had previously confirmed the presence of pulmonary metastases in an additional 20 mice in a preliminary experiment in advance. We also confirmed that there were no viable cells after cryotreatment using liquid nitrogen, in agreement with a previous study [35]. We observed no recurrence of the tumor at the primary site of inoculation after excision. All experiments were performed under the guidelines for animal experiments as stipulated by the Kanazawa University Graduate School of Medical Science [37].

LM8 cells, derived from Dunn osteosarcoma, were provided by the Riken BioResource Center (Saitama, Japan). The cells were maintained in complete medium consisting of RPMI 1640 supplemented with 10% heat-inactivated fetal bovine serum, 100 μg streptomycin per mL, and 100 units penicillin per mL and were cultured at 37°C in 5% CO_2. To establish local implantation of the tumor and subsequent lung metastasis, the LM8 cells (1×10^6) were suspended in 0.2 mL phosphate-buffered saline (PBS) and subcutaneously inoculated into the right

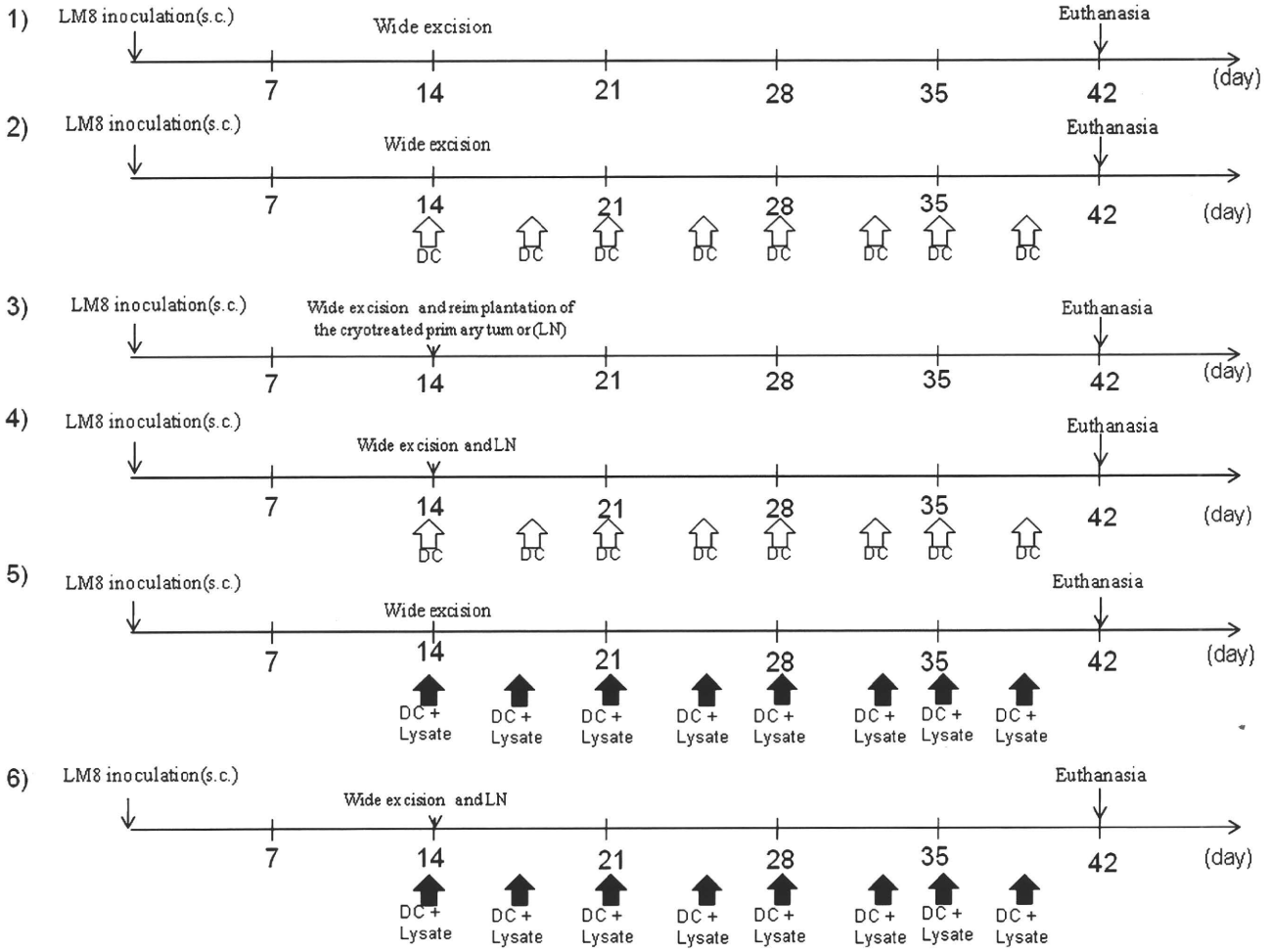

Fig. 1 A diagram of the experimental protocol and treatment schedule is shown. Two weeks after tumor inoculation, tumors were treated by one of the following methods: (1) excision only (n = 15); (2) DCs without reimplantation of the cryotreated primary tumor (n = 15); (3) reimplantation of the cryotreated primary tumor (n = 15); (4) DCs pulsed with cryotreated tumor lysates and reimplantation of the cryotreated primary tumor (n = 15); (5) DCs pulsed with cryotreated tumor lysates without reimplantation of the cryotreated primary tumor (n = 15); or (6) DCs pulsed with cryotreated tumor and reimplantation of the cryotreated primary tumor (LN) (n = 15). The mice were euthanized and evaluated 6 weeks after tumor inoculation. sc = subcutaneous.

gluteal region of the mice. All animals had macroscopically and microscopically confirmed lung metastases within 4 weeks [1].

C3H mice were purchased from Sankyo Labo Inc (Toyama, Japan) and housed in a specific pathogen-free animal facility in our laboratory. We were not able to accurately determine the survival time of each group because the guidelines for animal experiments concerning pain required euthanasia in distressed animals.

Liquid nitrogen (−196°C) was used for cryotreatment. Tumor tissue was collected on gauze and soaked in liquid nitrogen for 20 minutes for en bloc tumor tissue freezing. The tumor was prethawed at room temperature (20°C) for 15 minutes and then thawed in distilled water (20°C) for 15 minutes. The liquid nitrogen-treated tumor tissue was transplanted subcutaneously in the left gluteal region of the same mouse.

Because the mice were genetically identical, the structure of the major histocompatibility complex (MHC) Class I molecules was such that the T cells would be able to recognize the MHC Class I with antigens on the antigen-presenting cells (APCs) [17, 27]. Bone marrow-derived DCs were generated as described by Lutz and Rössner [28] with minor modifications. Briefly, erythrocyte-depleted mouse bone marrow cells obtained from flushed marrow cavities (1×10^6 cells/mL) were cultured in complete medium with 20 ng/mL recombinant mouse GMCSF (PeproTech EC Ltd, London, UK) in 10-cm tissue culture dishes at 37°C in an atmosphere containing 50 mL CO_2 per L. On Days 3 and 6, half of the medium was added to the

same volume of fresh complete medium and used to replenish the original plates. The freeze-thawed tumor lysate was added to the DC cultures on Day 6 at a ratio of five DC equivalents to one tumor cell (ie, 5:1) and incubated at 37°C in an atmosphere containing 50 mL CO_2 per L. After 24 hours of incubation, nonadherent cells including DCs were harvested by gentle pipetting.

For fluorescence activated cell sorting (FACS) analysis, DCs were counted with a FACSCalibur™ Flow Cytometer (Becton-Dickinson, San Jose, CA) and stained with fluorochrome-conjugated antibodies (BD Pharmingen, Tokyo, Japan) for the following markers: cluster of differentiation (CD)11c, CD80, CD86, I-Ad, and CD40. CD11c was used as a marker for all DCs regardless of the degree of maturation, whereas CD80, CD86, I-Ad, and CD40 are markers for DCs. Data analysis was performed with CELLQuest™ software (Becton-Dickinson). The corresponding labeled isotype antibodies served as controls. DCs used for vaccination were washed twice, enumerated, and resuspended in PBS at 1×10^6/mL.

We inoculated LM8 cells (5×10^6) in a mouse to make the tumor lysate. After 4 weeks, we resected the tumor mass and soaked the entire tumor in liquid nitrogen to kill the tumor cells. We mixed cryonecrotic tissue with DCs at Culture Day 6, after the tumor was defrosted, and the homogenate was prepared using PBS. The homogenate was passed through a 0.2-μm filter to remove bacteria and tissues and mixed with the DCs for 24 hours.

After intraperitoneal injection of 5 mL sodium pentobarbital (Somnopentyl®; Kyontsu Seiyaku, Tokyo, Japan), mice were euthanized by cervical dislocation and their blood was collected. Murine interferon (IFN)-γ and interleukin (IL)-4 release were measured by ELISA using Quantikine® (R & D Systems, Minneapolis, MN) according to the manufacturer's protocol using an Easy Reader EAR340 microtest plate reader (SLT-Labinstruments, Salzburg, Austria).

We estimated the area of the pulmonary metastatic lesion on 50 serial histologic sections of each lung by manually drawing orthogonal lines delimiting the edges of the pulmonary metastatic lesion and selected the widest part of the specimen. The area was determined by multiplying the maximum orthogonal dimensions using ImageJ software (NIH, Bethesda, MD; http://rsb.info.nih.gov/ij/). We compared the mean areas between the six groups.

For immunohistochemistry, lung specimens were fixed in 20% formalin and embedded in paraffin. For each case, we examined all the blocks of lung tissues of formalin-fixed, paraffin-embedded tumor tissue. All specimens were decalcified, although we found the decalcification step did not influence the immunohistochemistry for any of the stains. Five sections for each mouse were cut 4-μm thick. Each section was cut at the maximum diameter. CD8(+) T lymphocytes and natural killer (NK) cells in the pulmonary metastatic lesion were quantified by measuring the immunohistochemistry-positive cells per unit area in each group. Rehydrated tissue sections were incubated with rat monoclonal antibody raised against CD8(+) T lymphocytes of mouse origin (Santa Cruz Biotechnology, Santa Cruz, CA) and rat monoclonal antibody raised against NK cells of mouse origin (Abcam Plc, Cambridge, UK). The two antibodies were diluted 1:50 with PBS. Color reactions were performed at room temperature for 15 minutes and cover slips were mounted with glycerol and gelatin.

We determined differences in serum IFN-γ, serum IL-4, pulmonary metastatic area, and number of CD8(+) lymphocytes and NK cells in the metastatic area among the six groups using a nonrepeated-measures ANOVA and the Scheffe test. All analyses were conducted with SPSS® 11.0 software (SPSS Japan Inc, Tokyo, Japan).

Results

We activated antitumor immunity by combining DCs exposed to lysates of cryotreated tumor and reimplantation of the cryotreated primary tumor. On Culture Day 7, the ratio of mature DCs to immature DCs was increased compared with the ratio at Culture Day 6 (Fig. 2; immature DCs, upper left; mature DCs, upper right). Moreover, this increase was more apparent in groups incubated with tumor lysate. Serum IFN-γ levels were greater ($p < 0.0001$) in the mice that received DCs combined with reimplantation of the cryotreated primary tumor (119.0 ± 7.61 pg/mL) than in the cryotreated primary tumor alone group (37.33 ± 2.58 pg/mL). Moreover, the group that received tumor lysate-exposed DCs combined with reimplantation of the cryotreated primary tumor (157.33 ± 14 pg/mL) had a greater ($p < 0.0001$) IFN-γ level than the group that received only tumor lysate-exposed DCs without reimplantation of the cryotreated primary tumor (120.27 ± 11.29 pg/mL) (Fig. 3). Serum IL-4 was lower ($p < 0.0001$) in the mice that received DCs exposed to the lysates of cryotreated tumor and reimplantation of the cryotreated primary tumor group (13.33 ± 9.75 pg/mL) than in the excision-only group (45.06 ± 5.71 pg/mL) (Fig. 4).

The enhanced immune response by T lymphocytes reduced metastatic lesions. Reduction of the metastatic area was greater ($p < 0.0001$) in the group that received DCs without reimplantation of the cryotreated primary tumor (15.99 ± 3.93 mm^2) than in the excision-only group (24.12 ± 3.60 mm^2). The reduction of the metastatic area was greater ($p < 0.0001$) in the DCs combined with reimplantation of the cryotreated primary tumor group (5.39 ± 1.49 mm^2) than in the reimplantation of

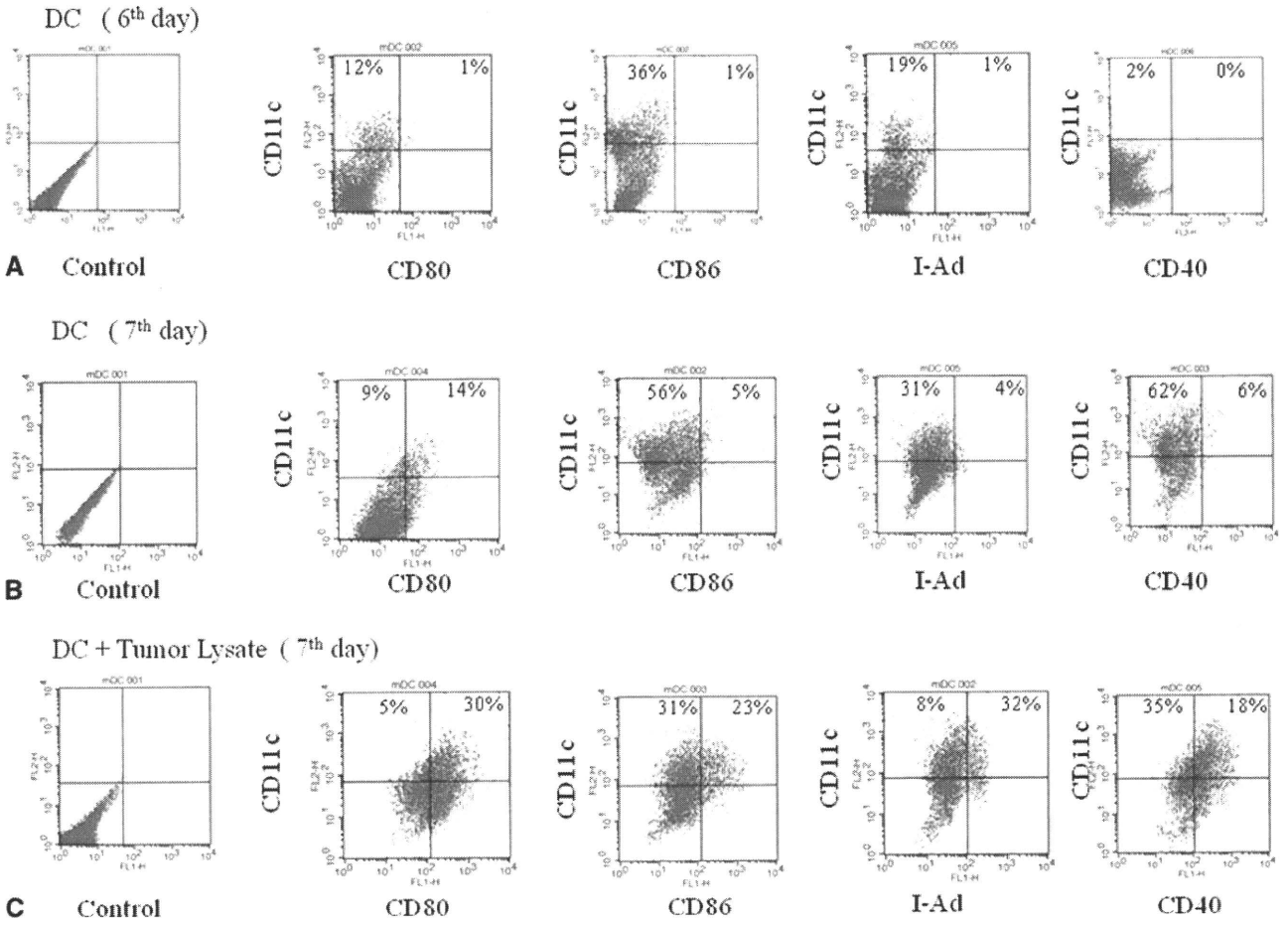

Fig. 2A–C DC activation status was examined using flow cytometry. DCs at Culture Day 7 (Group **B**) were more mature than DCs at Culture Day 6 (Group **A**). On Culture Day 7, DC maturity was greatest in the groups receiving lysate-primed DCs (Group **C**) than in those not receiving lysate-primed DCs (Group **B**).

Fig. 3 A graph of the serum IFN-γ levels in the six treatment groups is shown. The samples were collected 28 days after the reimplantation surgery and/or DC adoptive transfer. Mice that received DCs exposed to the lysates of cryotreated tumor and reimplantation of the cryotreated primary tumor group showed a highest IFN-γ level. Error bars represent SD.

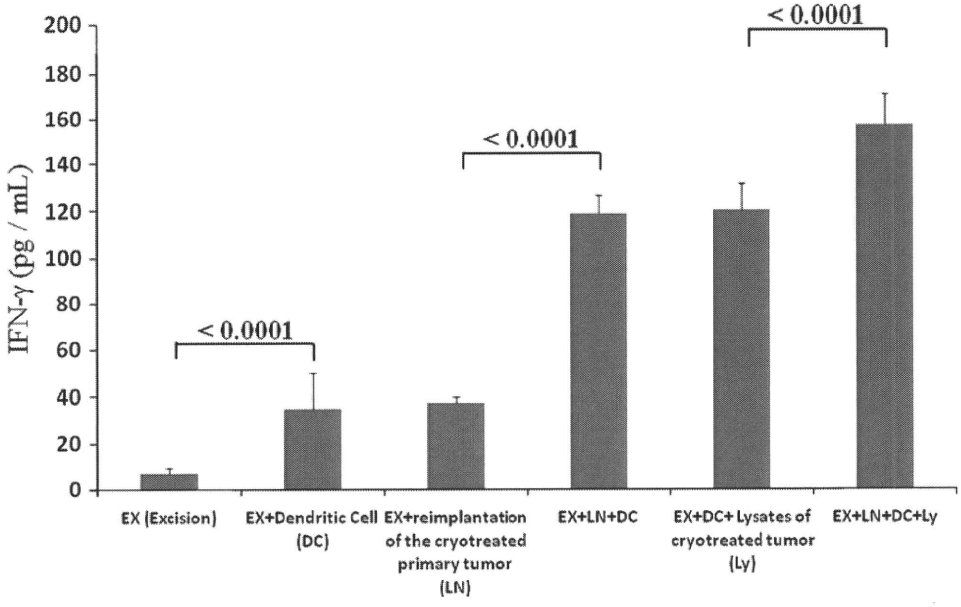

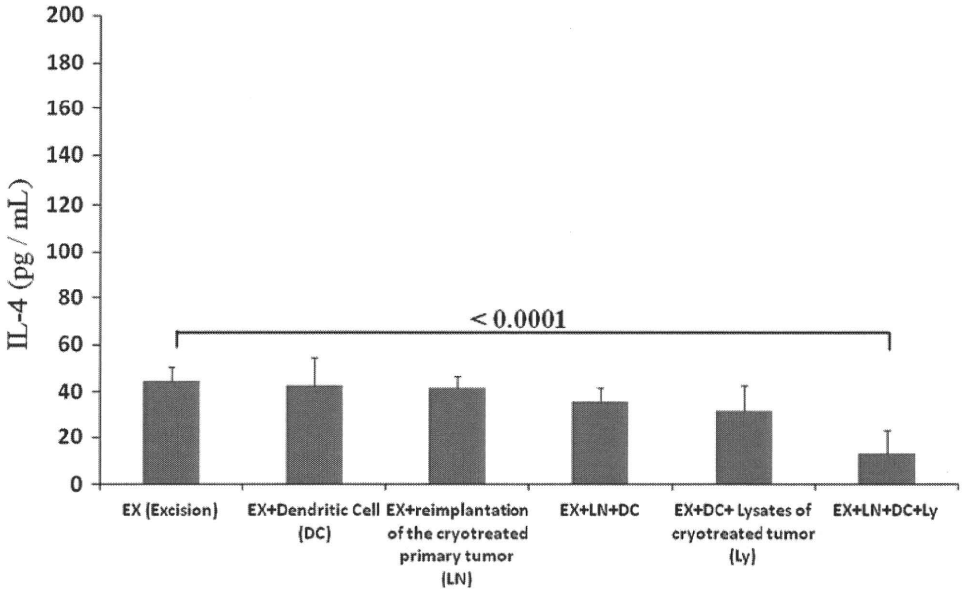

Fig. 4 A graph of the serum IL-4 in the six treatment groups is shown. Sera were collected 28 days after the reimplantation surgery and/or DC adoptive transfer. DCs exposed to the lysates of cryotreated tumor and reimplantation of the cryotreated primary tumor group showed a lower level than any of the other groups. Error bars represent SD.

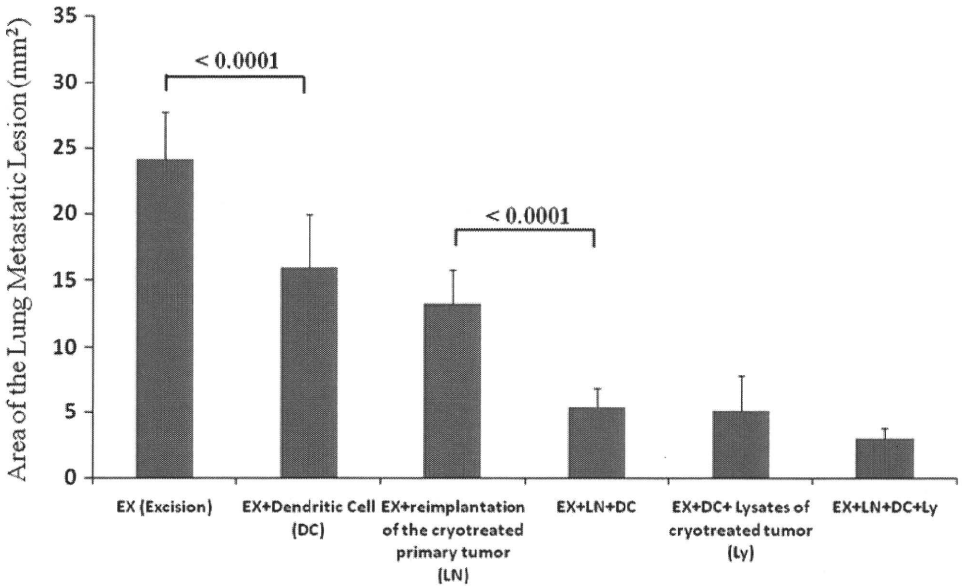

Fig. 5 Reduction of the metastatic area in the six treatment groups is shown. The samples were gathered 28 days after the reimplantation surgery and/or DC adoptive transfer. Error bars represent SD.

the cryotreated primary tumor alone group (13.22 ± 2.59 mm^2) (Fig. 5). CD8(+) T lymphocytes gathered in the pulmonary metastatic area in DC-treated groups, however, NK cells were not recruited to the metastatic area in the DC-treated groups compared with the nonDC-treated groups (Fig. 6). The number of CD8(+) T lymphocytes per unit area was greater ($p < 0.0001$) in the DCs combined with reimplantation of the cryotreated primary tumor group (8.33 ± 2.57 cells/mm^2) than in the reimplantation of the cryotreated primary tumor alone group (2.44 ± 0.53 cells/mm^2). Mice that received DCs exposed to the lysates of cryotreated tumor and reimplantation of the cryotreated primary tumor (12.79 ± 2.14 cells/mm^2) showed higher ($p < 0.0001$) levels than the group that received DCs exposed to the lysates of cryotreated tumor without reimplantation of the cryotreated primary tumor (8.71 ± 2.39 cells/mm^2) (Fig. 7). The number of NK cells per unit area was greater ($p < 0.0001$) in the group that received DCs exposed to the lysates of cryotreated tumor without reimplantation of the cryotreated primary tumor (3.90 ± 2.17 cells/mm^2) than in the excision-only group (1.20 ± 0.30 cells/mm^2) (Fig. 8). The CD8(+)T lymphocyte, CD4(+) T lymphocyte, and DC infiltrations in reimplanted tumors were similar to those seen with pulmonary metastases (data not shown).

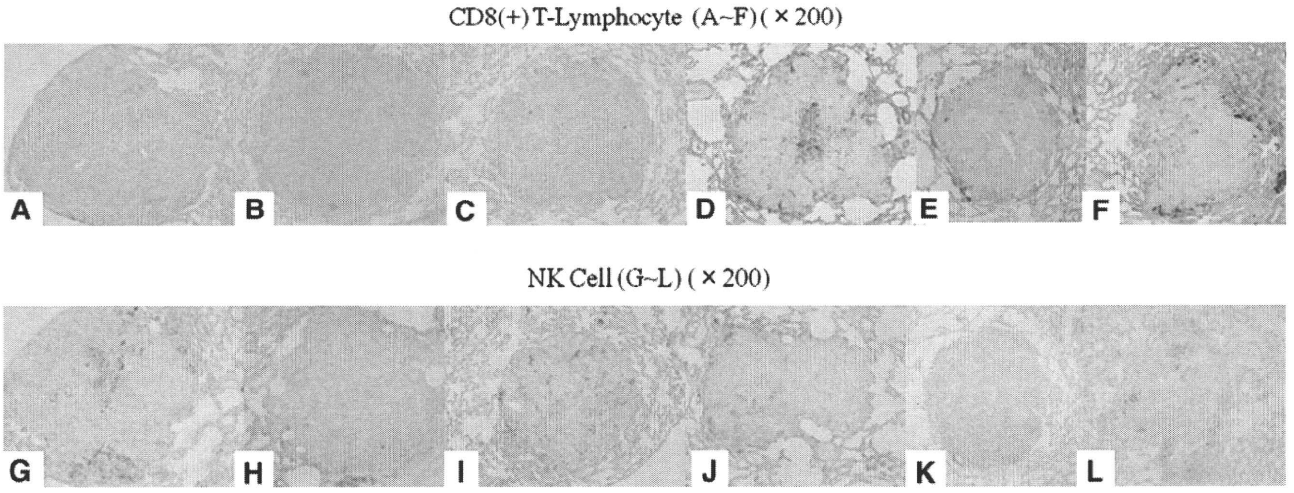

Fig. 6A–L To evaluate CD8(+) T lymphocytes and NK cells in pulmonary metastasis, immunostaining was performed: (**A**) CD8(+) T lymphocytes in Group 1, (**B**) CD8(+) T lymphocytes in Group 2, (**C**) CD8(+) T lymphocytes in Group 3, (**D**) CD8(+) T lymphocytes in Group 4, (**E**) CD8(+) T lymphocytes in Group 5, (**F**) CD8(+) T lymphocytes in Group 6, (**G**) NK cells in Group 1, (**H**) NK cells in Group 2, (**I**) NK cells in Group 3, (**J**) NK cells in Group 4, (**K**) NK cells in Group 5, and (**L**) NK cells in Group 6. CD8(+) T lymphocytes gathered in Groups D,E, and F. However, they did not gather in Groups A, B, and C. However, NK cells were recruited only in Groups A, B, and C. (Original magnification, ×200).

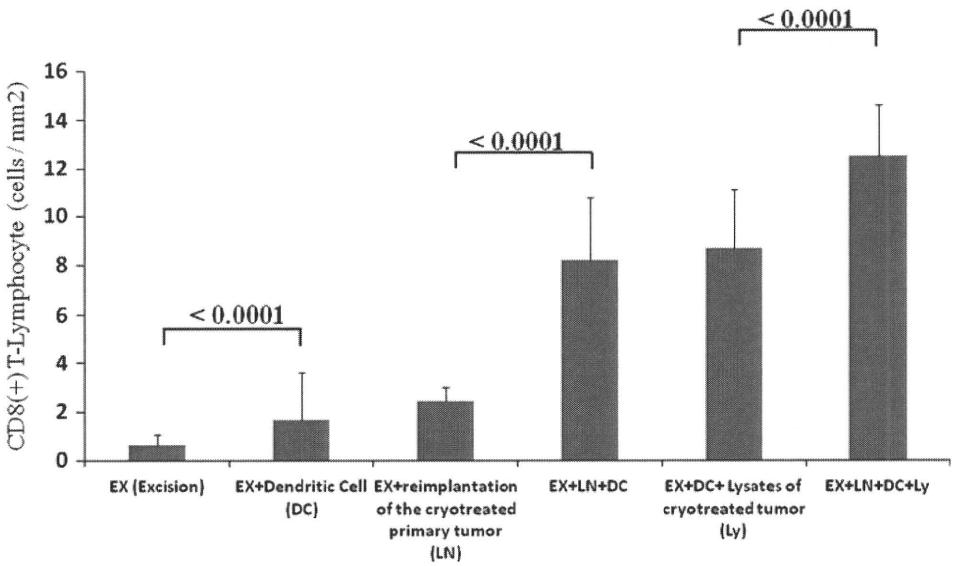

Fig. 7 The numbers of CD8(+) T lymphocytes per unit area in the six treatment groups are shown. The samples were gathered 28 days after the reimplantation surgery and/or DC adoptive transfer. DCs exposed to the lysates of cryotreated tumor and reimplantation of the cryotreated primary tumor group showed a higher level than any other groups. Error bars represent SD.

Discussion

Various immunotherapies for osteosarcoma have been tried. As standard treatments for osteosarcoma are ineffectual for many patients, new treatments need to be developed. In the 1970s, immunotherapy for osteosarcoma was reported by Southam et al. [42], Neff and Enneking [34], and Campbell et al. [5]. In the 1980s, new methods such as the use of interferons and Bacille de Calmette et Guérin were reported [22, 24, 36]. Another approach used antiidiotypic antibodies using T cells and liposome encapsulation [18, 51, 52]. Current methods of immunotherapy for osteosarcoma include peptide therapy or gene transfer therapy combined with hyperthermia therapy [10, 15, 21, 25, 33]. We asked whether (1) antitumor immunity could be achieved through activation of DCs combined with reimplantation of the cryotreated primary tumor and (2) if metastatic lesions would be prevented owing to enhanced T lymphocyte involvement.

We acknowledge limitations in this study. First, we used mice with an identical genetic makeup. The structure of the MHC Class I molecules was similar and the T cells could recognize the MHC Class I. However, we needed to use DCs from a different (albeit genetically identical) mouse to

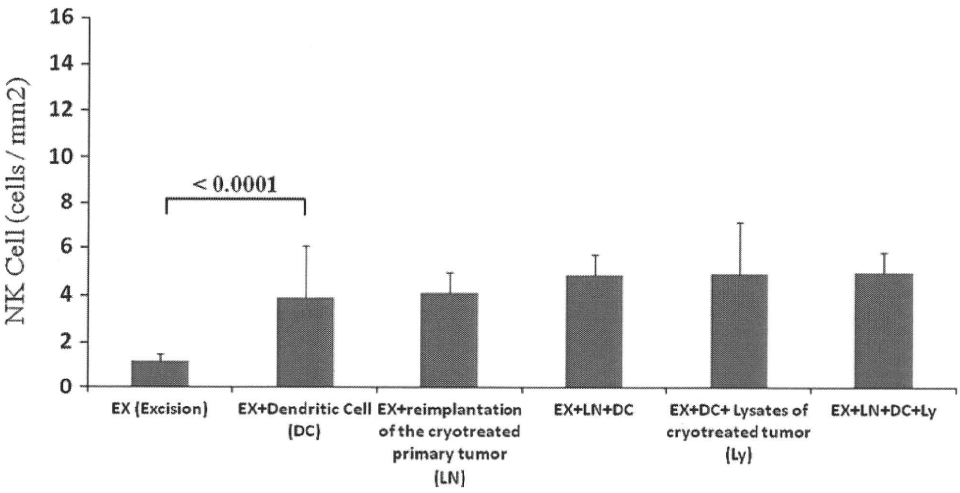

Fig. 8 The numbers of NK cells per unit area in the six treatment groups are shown. The samples were gathered 28 days after the reimplantation surgery and/or DC adoptive transfer. Error bars represent SD.

accomplish our adoptive transfer experiments. We minimized the potential for an immune response to nonself antigens by using genetically identical tumor tissue and mice. It would be necessary to use DCs derived from the same individual in clinical application, but this could not be achieved in our mouse model. In humans, however, monocytes are separated from the patient's own peripheral blood and DCs can be induced from these monocytes. Second, we could not completely replicate the clinical approach used in humans in our mouse model. In clinical cases frozen bone always is returned to the same site. However, it was impossible to replicate this in our experimental mouse model in which transplanted tumor cells were removed from the tibia and then returned to the same place after cryotreatment. In a preliminary experiment we attempted to do just that and these 20 mice could not move and died of starvation. We therefore used the contralateral gluteal region to check for local recurrence after tumor excision or recurrence from frozen tissue.

Antitumor immunity appeared to be activated through DCs combined with reimplantation of the cryotreated primary tumor or by exposing the transferred DC to lysates of cryotreated tumor. The use of lymphokine-activated killer (LAK) therapy has been used with other types of tumors [26]. However, T lymphocytes, which are the effectors, do not accumulate inside osteosarcoma tumors as expected. Autoclaving supplemented by DCs is thought to enhance the antitumor effect, but hyperthermia causes proteins to denature, and activation of the antitumor effect is often insufficient [37]. Several studies [12, 31, 41] report peptide vaccine therapy, but many patients apparently develop immunotolerance [45]. Thus, immunotherapy for malignant tumor achieved by these various methods has not been established definitively although investigations continue to try to overcome the major hurdles associated with immunotherapy (Table 1). We emphasize the immune response is activated by cryotreatment but not by heat-treated tissue. Our method differs from those described by others [7, 9, 10, 14]. In some regards DCs are believed to be the principal APCs for initiating immune responses in vivo [32]. In comparison with other traditional adjunct therapeutic options for cancer, such as radiation therapy and chemotherapy, immunotherapy provides a more targeted treatment to the cancer, with potentially fewer detrimental effects on noncancerous cells [30, 40]. DCs without sufficient cancer antigens may not have the ability to kill tumor cells and present the antigen to T lymphocytes by themselves. Our data suggest the antitumor effect in the group that received DCs without reimplantation of cryotreated primary tumor was almost the same as that in the reimplantation of cryotreated primary tumor alone group. The data further suggest the effects increased only when exposing the DCs to tumor lysates in the absence of cryonecrotic primary tumors. However, combining reimplantation of cryotreated primary tumor and DCs exposed to cryotreated tumor lysates produced synergistic effects. Using reimplantation of cryotreated primary tumor is more appropriate for clinical applications. We therefore believe an efficient immune response will be activated when DCs recognize tumor antigens appropriately. CD8(+) T cells act as an effector by the Th1 route, and this is promoted mainly by IFN-γ and IL-12 [38]. However, IL-4 [21], IL-6, and IL-10 strengthen humoral immunity. Levels of IFN-γ, IL-2, and IL-12 generally increase when cell-mediated immunity is activated, and IL-4, IL-6, and IL-10 increase when humoral immunity is activated. These cytokines act in opposition to maintain an immune balance.

Our data suggest enhanced T lymphocyte recruitment and function reduce metastatic lesions in a murine osteosarcoma model. Immunoreactivity increased slightly in mice that received DCs exposed to lysates of cryotreated tumor combined with reimplantation of the cryotreated primary tumor. NK cells attack the tumor independently of APCs. NK cells attack cells that downregulate MHC Class

Table 1. Immunotherapeutic trials of malignant tumors

Tumor	Immune intervention	Route	Immunologic response	Comments	References
Osteosarcoma	BCG	SC	NC	No consistent clinical effect	[22, 24]
Osteosarcoma	Interferon α	SC, IV	PR–NC	Osteosarcoma-associated antigens have potential for targeted immunotherapy	[36]
Unknown	LAK	IV	NC	T lymphocytes were unable to penetrate the tumor	[26]
Osteosarcoma	Antiidiotypic antibodies	IV	NC	It may be possible to circumvent this heterogeneity by activation of tissue macrophages to the tumoricidal state	[18, 51, 52]
Breast cancer, osteosarcoma	Peptide therapy combined with hyperthermia therapy	SC, IV	NC	It may be a potential agent for use in immunotherapy	[15, 20]
Osteosarcoma	Gene transfer therapy combined with hyperthermia therapy	IV	NC	IL-23 seems to be a less effective immunotherapeutic for adjuvant treatment of osteosarcomas	[25, 33]
Unknown	Peptide vaccine therapy	SC	NC–PD	Many patients have peptide-induced tolerance develop	[45]
Osteosarcoma	Cryoimmunology and DCs	SC	PR	Combining cryotreatment with DCs resulted in enhanced antitumor effects	Our data

BCG = Bacille de Calmette et Guérin; SC = subcutaneous; NC = no change; IV = intravenous; PR = partial response; LAK = lymphokine-activated killer; IL = interleukin; PD = progressive disease; DCs = dendritic cells.

I expression or have a stressed appearance [44]. We observed a reduced tumor burden in the groups that received transplanted DCs, which correlated with recruitment of CD8 lymphocytes to the tumor site as observed with immunohistochemistry.

Returning the frozen bone after liquid nitrogen treatment to its original place can be readily used in the clinic. After the first cryotreatment, it is possible to perform the treatment again using cultured DCs if a patient's tumor cells have been preserved. This approach therefore still can be used even after other methods (such as chemotherapy, radiation therapy, or surgery) no longer are reasonable. Combining DCs pulsed with lysates of cryotreated tumor and reimplantation of the cryotreated primary tumor enhanced antitumor effects. We believe the approach may be a useful alternative for patients with osteosarcoma when other treatment options including chemotherapy, radiotherapy, and surgical treatment have been ineffective.

Acknowledgments We thank Katsuro Tomita, Akihiko Takeuchi, Shuichi Kaneko, and Yohei Marukawa for supervision in this study.

References

1. Asai T, Ueda T, Itoh K, Yoshioka K, Aoki Y, Mori S, Yoshikawa H. Establishment and characterization of a murine osteosarcoma cell line (LM8) with high metastatic potential to the lung. *Int J Cancer.* 1998;76:418–422.
2. Bacci G, Lari S. Adjuvant and neoadjuvant chemotherapy in osteosarcoma. *Chir Organi Mov.* 2001;86:253–268.
3. Bielack SS, Kempf-Bielack B, Delling G, Exner GU, Flege S, Helmke K, Kotz R, Salzer-Kuntschik M, Werner M, Winkelmann W, Zoubek A, Jürgens H, Winkler K. Prognostic factors in high-grade osteosarcoma of the extremities or trunk: an analysis of 1,702 patients treated on neoadjuvant cooperative osteosarcoma study group protocols. *J Clin Oncol.* 2002;20:776–790.
4. Brewer WH, Austin RS, Capps GW, Neifeld JP. Intraoperative monitoring and postoperative imaging of hepatic cryosurgery. *Semin Surg Oncol.* 1998;14:129–155.
5. Campbell CJ, Cohen J, Enneking WF. Editorial: New therapies for osteogenic sarcoma. *J Bone Joint Surg Am.* 1975;57:143–144.
6. Chin JL, Lim D, Abdelhady M. Review of primary and salvage cryo-ablation for prostate cancer. *Cancer Control.* 2007;14:231–237.
7. DeLaney TF, Park L, Goldberg SI, Hug EB, Liebsch NJ, Munzenrider JE, Suit HD. Radiotherapy for local control of osteosarcoma. *Int J Radiat Oncol Biol Phys.* 2005;61:492–498.
8. de Moraes AM, Pavarin LB, Herreros F, de Aguiar Michelman F, Velho PE, de Souza EM. Cryosurgical treatment of lentigo maligna. *J Dtsch Dermatol Ges.* 2007;5:477–480.
9. Dinçbaş FO, Koca S, Mandel NM, Hiz M, Dervişoğlu S, Seçmezacar H, Oksüz DC, Ceylaner B, Uzel B. The role of preoperative radiotherapy in nonmetastatic high-grade osteosarcoma of the extremities for limb-sparing surgery. *Int J Radiat Oncol Biol Phys.* 2005;62:820–828.
10. Duparc J, Massin P, Bocquet L, Benfrech E, Cavagna R. [Autoclaved tumoral autografts: apropos of 12 cases, 6 of which highly malignant] [in French]. *Rev Chir Orthop Reparatrice Appar Mot.* 1993;79:261–271.
11. Enneking WF. A system for functional evaluation of the surgical management of musculoskeletal tumors. In: Enneking WF, ed. *Limb Salvage in Musculoskeletal Oncology.* New York, NY: Churchill-Livingstone; 1987:5–16.
12. Enomoto Y, Bharti A, Khaleque AA, Song B, Liu C, Apostolopoulos V, Xing PX, Calderwood SK, Gong J. Enhanced immunogenicity of heat shock protein 70 peptide complexes from

dendritic cell-tumor fusion cells. *J Immunol.* 2006;177:5946–5955.
13. Fagioli F, Biasin E, Mereuta OM, Muraro M, Luksch R, Ferrari S, Aglietta M, Madon E. Poor prognosis osteosarcoma: new therapeutic approach. *Bone Marrow Transplant.* 2008;41(suppl 2): S131–S134.
14. Harrington KD. The use of hemipelvic allografts or autoclaved grafts for reconstruction after wide resections of malignant tumors of the pelvis. *J Bone Joint Surg Am.* 1992;74:331–341.
15. Herbert LM, Grosso JF, Dorsey M Jr, Fu T, Keydar I, Cejas MA, Wreschner DH, Smorodinski N, Lopez DM. A unique mucin immunoenhancing peptide with antitumor properties. *Cancer Res.* 2004;64:8077–8084.
16. Hugate RR, Wilkins RM, Kelly CM, Madsen W, Hinshaw I, Camozzi AB. Intraarterial chemotherapy for extremity osteosarcoma and MFH in adults. *Clin Orthop Relat Res.* 2008;466:1292–1301.
17. Inaba K, Inaba M, Romani N, Aya H, Deguchi M, Ikehara S, Muramatsu S, Steinman RM. Generation of large numbers of dendritic cells from mouse bone marrow cultures supplemented with granulocyte/macrophage colony-stimulating factor. *J Exp Med.* 1992;176:1693–1702.
18. Killion JJ, Fidler IJ. Systemic targeting of liposome-encapsulated immunomodulators to macrophages for treatment of cancer metastasis. *Immunomethods.* 1994;4:273–279.
19. Koido S, Hara E, Homma S, Torii A, Mitsunaga M, Yanagisawa S, Toyama Y, Kawahara H, Watanabe M, Yoshida S, Kobayashi S, Yanaga K, Fujise K, Tajiri H. Streptococcal preparation OK-432 promotes fusion efficiency and enhances induction of antigen-specific CTL by fusions of dendritic cells and colorectal cancer cells. *J Immunol.* 2007;178:613–622.
20. Kubista B, Trieb K, Blahovec H, Kotz R, Micksche M. Hyperthermia increases the susceptibility of chondro- and osteosarcoma cells to natural killer cell-mediated lysis. *Anticancer Res.* 2002;22:789–792.
21. Kumaratilake LM, Ferrante A. IL-4 inhibits macrophage-mediated killing of Plasmodium falciparum in vitro: a possible parasite-immune evasion mechanism. *J Immunol.* 1992;149:194–199.
22. Larsson SE, Lorentzon R, Boquist L. Immunotherapy with irradiated tumour cells and BCG in experimental osteosarcoma. *Acta Orthop Scand.* 1981;52:469–474.
23. Lee JW, Kim H, Kang HJ, Kim HS, Park SH, Kim IO, Ahn HS, Shin HY. Clinical characteristics and treatment results of pediatric osteosarcoma: the role of high dose chemotherapy with autologous stem cell transplantation. *Cancer Res Treat.* 2008;40: 172–177.
24. Leventhal BG. Immunotherapy of sarcomas. *Natl Cancer Inst Monogr.* 1981;56:183–187.
25. Liebau C, Roesel C, Schmidt S, Karreman C, Prisack JB, Bojar H, Merk H, Wolfram N, Baltzer AW. Immunotherapy by gene transfer with plasmids encoding IL-12/IL-18 is superior to IL-23/IL-18 gene transfer in a rat osteosarcoma model. *Anticancer Res.* 2004;24:2861–2867.
26. Lotze MT, Line BR, Mathisen DJ, Rosenberg SA. The in vivo distribution of autologous human and murine lymphoid cells grown in T cell growth factor (TCGF): implications for the adoptive immunotherapy of tumors. *J Immunol.* 1980;125:1487–1493.
27. Lutz MB, Kukutsch N, Ogilvie AL, Rössner S, Koch F, Romani N, Schuler G. An advanced culture method for generating large quantities of highly pure dendritic cells from mouse bone marrow. *J Immunol Methods.* 1999;223:77–92.
28. Lutz MB, Rössner S. Factors influencing the generation of murine dendritic cells from bone marrow: the special role of fetal calf serum. *Immunobiology.* 2007;212:855–862.
29. Machak GN, Tkachev SI, Solovyev YN, Sinyukov PA, Ivanov SM, Kochergina NV, Ryjkov AD, Tepliakov VV, Bokhian BY, Glebovskaya VV. Neoadjuvant chemotherapy and local radiotherapy for high-grade osteosarcoma of the extremities. *Mayo Clin Proc.* 2003;78:147–155.
30. Meyers PA, Schwartz CL, Krailo M, Kleinerman ES, Betcher D, Bernstein ML, Conrad E, Ferguson W, Gebhardt M, Goorin AM, Harris MB, Healey J, Huvos A, Link M, Montebello J, Nadel H, Nieder M, Sato J, Siegal G, Weiner M, Wells R, Wold L, Womer R, Grier H. Osteosarcoma: a randomized, prospective trial of the addition of ifosfamide and/or muramyl tripeptide to cisplatin, doxorubicin, and high-dose methotrexate. *J Clin Oncol.* 2005; 23:2004–2011.
31. Monzavi-Karbassi B, Hennings LJ, Artaud C, Liu T, Jousheghany F, Pashov A, Murali R, Hutchins LF, Kieber-Emmons T. Preclinical studies of carbohydrate mimetic peptide vaccines for breast cancer and melanoma. *Vaccine.* 2007;25:3022–3031.
32. Morikawa Y, Tohya K, Ishida H, Matsuura N, Kakudo K. Different migration patterns of antigen-presenting cells correlate with Th1/Th2-type responses in mice. *Immunology.* 1995;85: 575–581.
33. Nakashima Y, Deie M, Yanada S, Sharman P, Ochi M. Magnetically labeled human natural killer cells, accumulated in vitro by an external magnetic force, are effective against HOS osteosarcoma cells. *Int J Oncol.* 2005;27:965–971.
34. Neff JR, Enneking WF. Adoptive immunotherapy in primary osteosarcoma: an interim report. *J Bone Joint Surg Am.* 1975; 57:145–148.
35. Nishida H, Tsuchiya H, Tomita K. Re-implantation of destructive tumour tissue treated by liquid nitrogen cryotreatment induces anti-tumour activity against murine osteosarcoma. *J Bone Joint Surg Br.* 2008;90:1249–1255.
36. Pelham JM, Gray JD, Flannery GR, Pimm MV, Baldwin RW. Interferon-alpha conjugation to human osteogenic sarcoma monoclonal antibody 791T/36. *Cancer Immunol Immunother.* 1983;15:210–216.
37. Research Promotion Bureau, Life Sciences Divisions. Fundamental guidelines for proper conduct of animal experiments and related activities in academic research institutions under the jurisdiction of the Ministry of Education, Culture, Sports, Science and Technology. Ministry of Education, Culture, Sports, Science and Technology, Notice No. 71. Available at: http://www.lifescience.mext.go.jp/policies/pdf/an_material011.pdf. Accessed October 29, 2007.
38. Romieu R, Baratin M, Kayibanda M, Guillet JG, Viguier M. IFN-gamma-secreting Th cells regulate both the frequency and avidity of epitope-specific CD8 + T lymphocytes induced by peptide immunization: an ex vivo analysis. *Int Immunol.* 1998;10:1273–1279.
39. Sabel MS, Kaufman CS, Whitworth P, Chang H, Stocks LH, Simmons R, Schultz M. Cryoablation of early-stage breast cancer: work-in-progress report of a multi-institutional trial. *Ann Surg Oncol.* 2004;11:542–549.
40. Schendel DJ, Gansbacher B, Oberneder R, Kriegmair M, Hofstetter A, Riethmüller G, Segurado OG. Tumor-specific lysis of human renal cell carcinomas by tumor-infiltrating lymphocytes. I. HLA-A2-restricted recognition of autologous and allogeneic tumor lines. *J Immunol.* 1993;151:4209–4220.
41. Slingluff CL Jr, Chianese-Bullock KA, Bullock TN, Grosh WW, Mullins DW, Nichols L, Olson W, Petroni G, Smolkin M, Engelhard VH. Immunity to melanoma antigens: from self-tolerance to immunotherapy. *Adv Immunol.* 2006;90:243–295.
42. Southam CM, Marcove R, Shanks E. Clinical trials of autogenous tumor vaccine for treatment of osteogenic sarcoma. *Proceedings of the Seventh National Cancer Conference.* Philadelphia, PA: JB Lippincott; 1973:91.

43. Tanzawa Y, Tsuchiya H, Yamamoto N, Sakayama K, Minato H, Tomita K. Histological examination of frozen autograft treated by liquid nitrogen removed 6 years after implantation. *J Orthop Sci.* 2008;13:259–264.
44. Terunuma H, Deng X, Dewan Z, Fujimoto S, Yamamoto N. Potential role of NK cells in the induction of immune responses: implications for NK cell-based immunotherapy for cancers and viral infections. *Int Rev Immunol.* 2008;27:93–110.
45. Toes RE, Blom RJ, Offringa R, Kast WM, Melief CJ. Enhanced tumor outgrowth after peptide vaccination: functional deletion of tumor-specific CTL induced by peptide vaccination can lead to the inability to reject tumors. *J Immunol.* 1996;156:3911–3918.
46. Tsuchiya H, Tomita K, Mori Y, Asada N, Morinaga T, Kitano S, Yamamoto N. Caffeine-assisted chemotherapy and minimized tumor excision for nonmetastatic osteosarcoma. *Anticancer Res.* 1998;18:657–666.
47. Tsuchiya H, Tomita K, Mori Y, Asada N, Yamamoto N. Marginal excision for osteosarcoma with caffeine assisted chemotherapy. *Clin Orthop Relat Res.* 1999;358:27–35.
48. Tsuchiya H, Wan SL, Sakayama K, Yamamoto N, Nishida H, Tomita K. Reconstruction using an autograft containing tumour treated by liquid nitrogen. *J Bone Joint Surg Br.* 2005;87:218–225.
49. Tsuchiya H, Yasutake H, Yokogawa A, Baba H, Ueda Y, Tomita K. Effect of chemotherapy combined with caffeine for osteosarcoma. *J Cancer Res Clin Oncol.* 1992;118:567–569.
50. Urano M, Tanaka C, Sugiyama Y, Miya K, Saji S. Antitumor effects of residual tumor after cryoablation: the combined effect of residual tumor and a protein-bound polysaccharide on multiple liver metastases in a murine model. *Cryobiology.* 2003;46:238–245.
51. Visonneau S, Cesano A, Jeglum KA, Santoli D. Adjuvant treatment of canine osteosarcoma with the human cytotoxic T-cell line TALL-104. *Clin Cancer Res.* 1999;5:1868–1875.
52. Warren RQ, Tsang KY. Induction of immunity to a human osteosarcoma-associated antigen in mice using anti-idiotypic antibodies. *Clin Immunol Immunopathol.* 1990;56:334–343.
53. Yamamoto N, Tsuchiya H, Tomita K. Effects of liquid nitrogen treatment on the proliferation of osteosarcoma and the biomechanical properties of normal bone. *J Orthop Sci.* 2003;8:374–380.

Cancer Research

Antitumor Effect after Radiofrequency Ablation of Murine Hepatoma Is Augmented by an Active Variant of CC Chemokine Ligand 3/Macrophage Inflammatory Protein-1α

Noriho Iida[1], Yasunari Nakamoto[1], Tomohisa Baba[2], Hidetoshi Nakagawa[1], Eishiro Mizukoshi[1], Makoto Naito[3], Naofumi Mukaida[2], and Shuichi Kaneko[1]

Abstract

Several chemokines are used for immunotherapy against cancers because they can attract immune cells such as dendritic and cytotoxic T cells to augment immune responses. Radiofrequency ablation (RFA) is used to locally eliminate cancers such as hepatocellular carcinoma (HCC), renal cell carcinoma, and lung cancer. Because HCC often recurs even after an eradicative treatment with RFA, additional immunotherapy is necessary. We treated tumor-bearing mice by administering ECI301, an active variant of CC chemokine ligand 3, after RFA. Mice were injected s.c. with BNL 1ME A.7R.1, a murine hepatoma cell line, in the bilateral flank. After the tumor became palpable, RFA was done on the tumor of one flank with or without ECI301. RFA alone eliminated the treated ipsilateral tumors and retarded the growth of contralateral non–RFA-treated tumors accompanied by massive T-cell infiltration. Injection of ECI301 augmented RFA-induced antitumor effect against non–RFA-treated tumors when administered to wild-type or *CCR5*-deficient but not *CCR1*-deficient mice. ECI301 also increased CCR1-expressing $CD11c^+$ cells in peripheral blood and RFA-treated tumors after RFA. Deficiency of *CCR1* impairs accumulation of $CD11c^+$, $CD4^+$, and $CD8^+$ cells in RFA-treated tumors. Furthermore, in IFN-γ-enzyme-linked immunospot assay, ECI301 augmented tumor-specific responses after RFA whereas deficiency of *CCR1* abolished this augmentation. Thus, we proved that ECI301 further augments RFA-induced antitumor immune responses in a CCR1-dependent manner. *Cancer Res; 70(16); 6556–65. ©2010 AACR.*

Introduction

Chemokines are a class of candidate molecules for immunotherapy. Chemokines are presumed to play an essential role in the regulation of leukocyte trafficking and dendritic cell-T-cell interactions (1–4). In animal experiments, intratumoral use of chemokines, such as monocyte chemoattractant protein-1/CC chemokine ligand 2 (CCL2), macrophage inflammatory protein (MIP)-1α/CCL3, or MIP-3α/CCL20, succeeds in decreasing tumorigenesis accompanied by increase in the numbers of tumor-infiltrating dendritic, natural killer, or T cells (5–7). Thus, application of chemokines in immunotherapy is promising but needs further refinement before they can be used in clinical situations.

Radiofrequency ablation (RFA) is an eradicative treatment against cancers, such as hepatocellular carcinoma (HCC), renal cell carcinoma, and lung cancer. RFA of HCC can generate HCC-specific T cells in peripheral blood (8). Activation of dendritic cells in human peripheral blood is also observed after this treatment (9). Thus, RFA can induce immunogenic tumor cell death and subsequently tumor-specific immune responses (8–11). However, multicentric development of HCC in the cirrhotic liver frequently results in tumor recurrence even after the apparent curative treatment of HCC by RFA (12). These observations suggest that RFA-induced tumor-specific immune responses are often not sufficient to prevent tumor recurrence. Thus, additional treatment modalities are required to augment HCC-specific immune responses.

CCL3/MIP-1α can augment immune responses but problems arise because of its tendency to form large aggregates at high concentrations when administered systemically. Unlike human naïve CCL3, BB-10010 is generated by a single amino acid substitution of Asp26 to Ala and exhibits similar biological potencies, but rarely forms large aggregates (13). Based on its activity to mobilize bone marrow cells to peripheral blood, randomized clinical trials were performed to examine whether the combined administration of BB-10010 and chemotherapeutic agents can protect against chemotherapy-induced neutropenia. However, the myeloprotective effects of BB-10010 were not sufficient to warrant its use with chemotherapy (14). Concomitantly, several lines of evidence reveal that the administration of human recombinant CCL3

Authors' Affiliations: [1]Disease Control and Homeostasis, Graduate School of Medical Science, and [2]Division of Molecular Bioregulation, Cancer Research Institute, Kanazawa University, Kanazawa, Japan; and [3]Division of Cellular and Molecular Pathology, Niigata University Graduate School of Medicine, Niigata, Japan

Corresponding Author: Shuichi Kaneko, Disease Control and Homeostasis, Graduate School of Medical Science, Kanazawa University, 13-1 Takara-machi, Kanazawa 920-8641, Japan. Phone: 81-76-265-2235; Fax: 81-76-234-4250; E-mail: skaneko@m-kanazawa.jp.

doi: 10.1158/0008-5472.CAN-10-0096

can mobilize activated T-cell and dendritic cell precursors into circulation (15, 16).

ECI301, which has the same amino acid sequence as BB-10010, was generated using the fission yeast (*Schizosaccharomyces pombe*) expression system. ECI301 can augment irradiation-induced tumor regression when administered systemically to mice bearing multiple subcutaneous tumors (17). Of interest is the fact that the effects were observed in both unirradiated and irradiated tumors. Thus, systemic ECI301 treatment can augment irradiation-induced tumor-specific systemic immunity. These observations prompted us to investigate the effects of ECI301 on RFA-treated mice. Here, we show that ECI301 further augments RFA-induced antitumor immune responses in a CCR1-dependent manner.

Materials and Methods

Mice

Seven- to 9-week-old specific pathogen–free female BALB/c mice were purchased from Charles River Japan and designated as wild-type (WT) mice. BALB/c-*nu/nu* mice were purchased from CLEA Japan. *CCR1*-deficient (*CCR1*$^{-/-}$) mice were a gift from Dr. Philip M. Murphy (National Institute of Allergy and Infectious Disease, NIH, Bethesda, MD); *CCR5*-deficient (*CCR5*$^{-/-}$) mice were a gift from Dr. Kouji Matsushima (Department of Molecular Preventive Medicine, Tokyo University, Tokyo, Japan). All mice were backcrossed to BALB/c mice for 8 to 10 generations. All animal experiments were performed under specific pathogen–free conditions in accordance with the Guidelines for the Care and Use of Laboratory Animals of Kanazawa University (Japan).

Tumor cell line

A murine HCC cell line, BNL 1ME A.7R.1 (BNL), was purchased from the American Type Culture Collection in 1998 and kept at low passage throughout the study. The cells were screened for bacteria, fungus, and *Mycoplasma* contamination by direct culture method in 2006 before start of the study. The cells were cultured in DMEM (Sigma Chemical Co.) containing 10% fetal bovine serum (FBS), 0.1 mmol/L nonessential amino acids, 1 μmol/L sodium pyruvate, 2 mmol/L L-glutamine, 50 μg/mL streptomycin, and 100 units/mL penicillin (Life Technologies, Inc.).

Animal models

ECI301 was generated as previously described and provided by Effector Cell Institute, Inc. (17, 18). The left and right flanks of 7- to 9-week-old female WT, *CCR1*$^{-/-}$, *CCR5*$^{-/-}$, and *nu/nu* mice were injected s.c. with 5×10^5 BNL cells in 100 μL of PBS. Fourteen days later, when tumor size reached a diameter of 6 to 8 mm, tumors of one flank were treated using a radiofrequency generator (RITA 500PA, RITA Medical Systems) and needle as described below. On days 0, 2, and 4 after RFA, 20 μg of ECI301 in 100 μL of PBS were injected i.v. via the tail vein, whereas mice treated with RFA alone were injected with 100 μL of PBS. Untreated tumor-bearing mice were used as controls. In another schedule, 2 μg of ECI301 in 100 μL of PBS were injected i.v. from day 0 to day 4 (5 consecutive days). The sizes of non–RFA-treated tumors on the contralateral flank were evaluated twice a week using calipers, and tumor volumes were calculated using the following formula: tumor volume (mm^3) = (longest diameter) × (shortest diameter)^2 / 2.

RFA-treated or non–RFA-treated tumors were excised at the indicated time intervals for immunohistochemical analysis and quantitative real-time reverse transcription-PCR (RT-PCR). Spleens and peripheral blood were removed from the mice at the indicated time intervals for flow cytometric analysis and enzyme-linked immunospot assay (ELISPOT).

Radiofrequency ablation

Mice were anesthetized by i.p. injection of Somnopentyl (Schering-Plough Animal Health) and carefully shaved in the tumor area. After placing the mice onto an aluminum plate attached with an electricity-conducting pad, an RFA needle of expandable electrode with maximum dimension of 20 mm (70SB 2 cm; RITA Medical Systems) was inserted into the middle of the tumors and expanded at 2 or 3 mm. RFA treatments were done using a radiofrequency generator at a power output of 25 W for 1.5 minutes and the temperature of the needle tips reached 70°C to 80°C.

Immunohistochemical analysis

The removed tumor tissues were embedded in Sakura Tissue-Tek optimum cutting temperature (OCT) compound (Sakura Finetek) as frozen tissues. Cryostat sections of the frozen tissues were fixed with 4% paraformaldehyde in PBS and stained with rat anti-mouse CD4 (BD Biosciences), rat anti-mouse CD8a (BD Biosciences), hamster anti-mouse CD11c (BD Biosciences), and rat anti-mouse F4/80 antibodies (Serotec) overnight at 4°C. The sections were then incubated with biotinylated rabbit anti-rat IgG (DakoCytomation) or biotinylated mouse anti-hamster IgG (BD Biosciences) for 1 hour at room temperature. The immune complexes were visualized using the Catalyzed Signal Amplification System (DakoCytomation) or the Vectastain Elite ABC and DAB substrate kits (Vector Laboratories) according to the manufacturer's instructions. As a negative control, rat IgG (Cosmo Bio) or hamster IgG (BD Biosciences) was used instead of specific primary antibodies. The numbers of positive cells in each animal were counted in 10 randomly selected fields at 400-fold magnification by an examiner without any prior knowledge of the experimental procedures.

Double-color immunofluorescence analysis

Tumor tissues were embedded in OCT compound as frozen tissues. After fixation with 4% paraformaldehyde/PBS, cryostat sections were stained with the combinations of anti-CD4 and goat anti-mouse CCR1 (Santa Cruz Biotechnology), anti-CD8a and anti-CCR1, anti-F4/80 and anti-CCR1, phycoerythrin (PE)-conjugated hamster anti-CD11c (BD Biosciences) and anti-CCR1, anti-F4/80 and goat anti-mouse CCL3 (R&D Systems), and anti-F4/80 and goat anti-mouse CCL4 antibodies (R&D). After extensive washing, AF488 donkey anti-rat IgG (Invitrogen) was used as a secondary antibody to detect $CD4^+$, $CD8a^+$, or $F4/80^+$ cells. Simultaneously,

AF546- or AF488-donkey anti-goat IgG (Invitrogen) was used to detect $CCR1^+$, $CCL3^+$, or $CCL4^+$ cells. The sections were observed using a confocal microscope (LSM 510 META, Zeiss).

Quantitative real-time RT-PCR

Total RNA was extracted from the resected tumor using RNeasy Mini Kit (Qiagen) according to the manufacturer's instructions. After treating the RNA preparations with RNase-free DNase I (Qiagen) to remove residual DNA, cDNA was synthesized as described previously (19). Quantitative real-time PCR was done on a StepOne Real-Time PCR System (Applied Biosystems) using the comparative C_T quantification method. TaqMan Gene Expression Assays (Applied Biosystems) containing specific primers and probes [accession numbers: CCL3, Mm00441258_ml; CCL4, Mm00443111_m1; CCL5, Mm01302428_ml; glyceraldehyde-3-phosphate dehydrogenase (GAPDH), Mm99999915_g1] and TaqMan Fast Universal PCR Master Mix were used with 10 ng of cDNA to quantify the expression levels of CCL3, CCL4, and CCL5. Reactions were performed for 20 seconds at 95°C followed by 40 cycles of 1 second at 95°C and 20 seconds at 60°C. GAPDH was amplified as an internal control and its C_T values were subtracted from the C_T values of the target genes (ΔC_T). The ΔC_T values of tumors after RFA with or without ECI301 were compared with the ΔC_T values of tumors of untreated mice.

Enzyme-linked immunospot assay

To prepare tumor lysates, BNL or CT26 cells were suspended in PBS and subjected to four cycles of rapid freezing in liquid nitrogen and thawing at 55°C. The lysate was spun at 15,000 rpm to remove particulate cellular debris. After harvesting murine spleens on day 21 after RFA, mononuclear cells were isolated by centrifugation through a Histopaque-1083 density gradient (Sigma Chemical). ELISPOT was performed using an IFN-γ-ELISPOT kit (Mabtech). Ninety-six-well plates coated with anti-mouse IFN-γ antibody were blocked for 2 hours with RPMI 1640 (Sigma Chemical) containing 10% FBS. Two hundred fifty thousand splenic mononuclear cells were added in triplicate cultures of RPMI 1640 containing 10% FBS together with BNL or CT26 lysates at a tumor cell-to-mononuclear cell ratio of 2:1. After 48 hours of culture, the plates were washed eight times with sterile PBS and further incubated for 2 hours with biotinylated anti-mouse IFN-γ antibody. After another eight washes, alkaline phosphatase–conjugated streptavidin was added to these

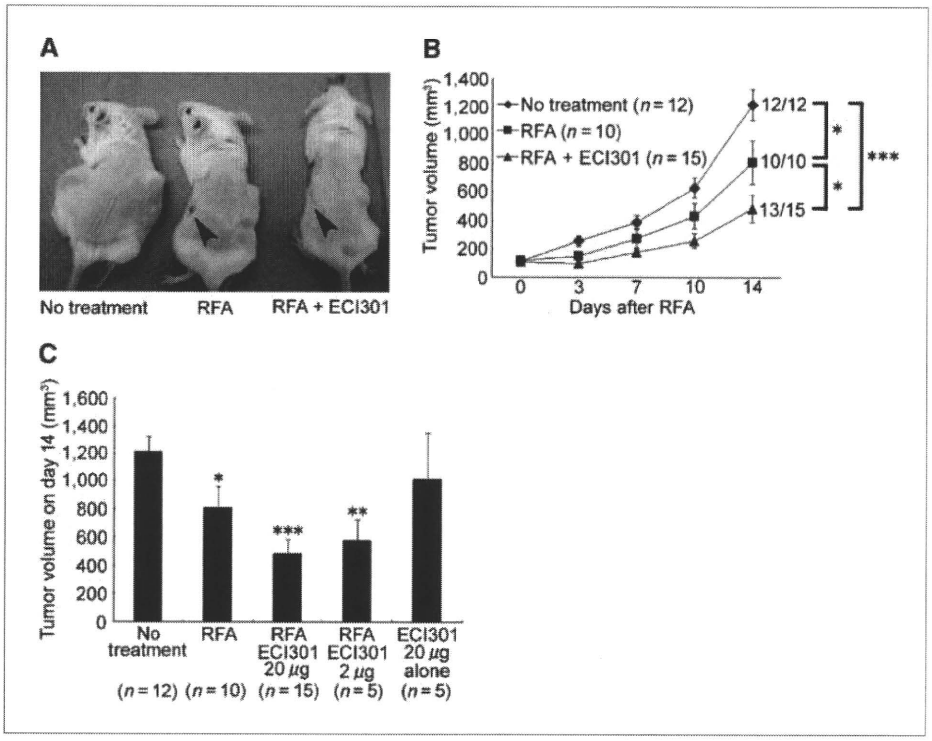

Figure 1. ECI301-induced augmentation of antitumor effects after RFA. WT mice were injected s.c. with 5×10^5 BNL cells into the left and right flanks. Fourteen days later, when tumors became palpable, tumors of one flank were treated using the RFA generator and needle. On day 0, 2, and 4 after RFA, 20 μg of ECI301 in 100 μL of PBS were injected i.v. into each mouse, whereas mice treated with RFA alone were injected with 100 μL of PBS. Tumor-bearing untreated mice were observed as controls. A, macroscopic appearances of the mice on day 14 after RFA are shown. Arrowheads indicate the scar after RFA. Representative results are from at least 10 mice in each group. B, non–RFA-treated tumor volumes after RFA with or without ECI301 were measured twice a week. Points, mean; bars, SE. *, $P < 0.05$; ***, $P < 0.001$. C, volumes of non–RFA-treated tumors on day 14 after RFA. In addition to the groups described in B, tumor volumes were determined in animals receiving 2 μg of ECI301 in 100 μL of PBS i.v. from day 0 to day 4 (5 consecutive days) after RFA and those receiving 20 μg of ECI301 alone without RFA. Columns, mean; bars, SE. *, $P < 0.05$; **, $P < 0.01$; ***, $P < 0.001$, compared with untreated mice.

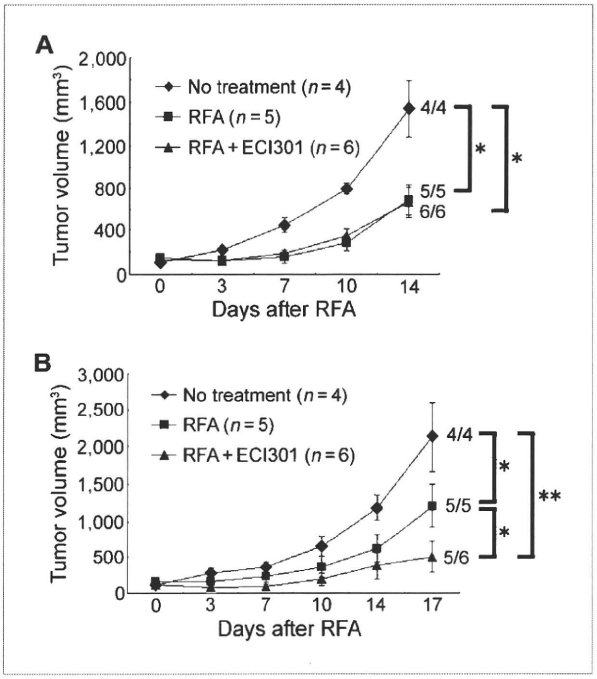

Figure 2. Deficiency of *CCR1* abrogates ECI301-augmented antitumor effects after RFA. *CCR1*$^{-/-}$ or *CCR5*$^{-/-}$ mice were inoculated with BNL cells and treated as described in the legend to Fig. 1. Non–RFA-treated tumor volumes were measured twice a week in *CCR1*$^{-/-}$ (A) and *CCR5*$^{-/-}$ (B) mice. Points, mean; bars, SE. *, $P < 0.05$; **, $P < 0.01$.

plates and incubated for 1 hour. Finally, the spots were developed with nitroblue tetrazolium/5-bromo-4-chloro-3-indolyl phosphate solution. The number of specific spots was determined by subtracting the number of spots in wells without lysates from the number of spots in wells with tumor lysates. Wells were considered positive if they had more than 10 spots per well and were at least 2-fold greater than control.

Flow cytometric analysis

After harvesting blood samples from mice, mononuclear cells were isolated by centrifugation through a Histopaque-1083 density gradient (Sigma Chemical). The resultant single-cell preparations were stained with various combinations of allophycocyanin (APC)-labeled anti-CD8, APC-labeled anti-CD11c, FITC-labeled anti-CD4 (BD Biosciences), PE-labeled anti-CCR1 (Santa Cruz Biotechnology), and FITC-labeled anti-F4/80 monoclonal antibodies (Serotec). APC-rat IgG, APC-hamster IgG, and FITC-rat IgG were used as isotype controls (BD Biosciences). For each determination, at least 20,000 stained cells were analyzed on a FACSCalibur system (BD Biosciences). The data were expressed as the proportion of positive cells (compared with cells stained with an irrelevant control antibody).

Depletion of macrophages/monocytes

Clodronate liposome was prepared and systemic depletion of monocytes/macrophages was performed as previously described (20, 21). WT mice were i.p. injected with 200 μL of clodronate liposome five times: days −2, 0, 3, 6, and 10 after RFA treatment. Depletion of CD11c-negative monocytes in blood was confirmed by flow cytometry after injection of clodronate liposome.

Statistical analysis

Mean and SD or SE were calculated for the obtained data. Data were analyzed statistically using one-way ANOVA followed by Fisher's protected least significant difference test, except for the data of tumor growth, which were analyzed with two-way ANOVA. $P < 0.05$ was considered statistically significant.

Results

ECI301 augments RFA-induced antitumor effects

To investigate the effects of RFA against RFA-treated and non–RFA-treated tumors, each bilateral flank of BALB/c mice was injected with 5×10^5 BNL cells. Fourteen days later, when tumor size reached a diameter of 6 to 8 mm, tumors of one flank were treated with RFA. On the day after RFA, ulceration occurred in RFA-treated tumors, and these tumors started to shrink (data not shown). On day 14 after RFA, RFA-treated tumors were covered with scars without any macroscopic tumors (Fig. 1A). Moreover, RFA treatment also retarded the growth of contralateral non–RFA-treated tumors compared with the tumors in untreated mice (Fig. 1B and C). ECI301 (20 μg/mouse) administered on days 0, 2, and 4 after RFA augmented RFA-induced growth retardation of contralateral non–RFA-treated tumors (Fig. 1B and C). Furthermore, non–RFA-treated tumors completely disappeared in 2 of 15 mice treated with RFA and ECI301 but not in the other treatment groups (Fig. 1B and C). Therapeutic effects were observed, even when ECI301 (2 μg/mouse) was injected consecutively for 5 days from day 0 to day 4 after RFA.

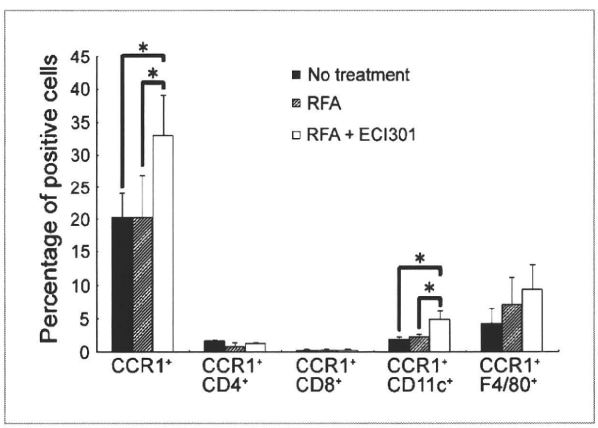

Figure 3. ECI301 increases CCR1-expressing cells in peripheral blood. Peripheral blood sample was harvested 8 h after RFA. Mononuclear cells were separated and stained with the indicated antibodies as described in Materials and Methods. Columns, mean percentages of CCR1$^+$, CCR1$^+$CD4$^+$, CCR1$^+$CD8$^+$, CCR1$^+$CD11c$^+$, or CCR1$^+$F4/80$^+$ cells ($n = 3$); bars, SD. *, $P < 0.05$.

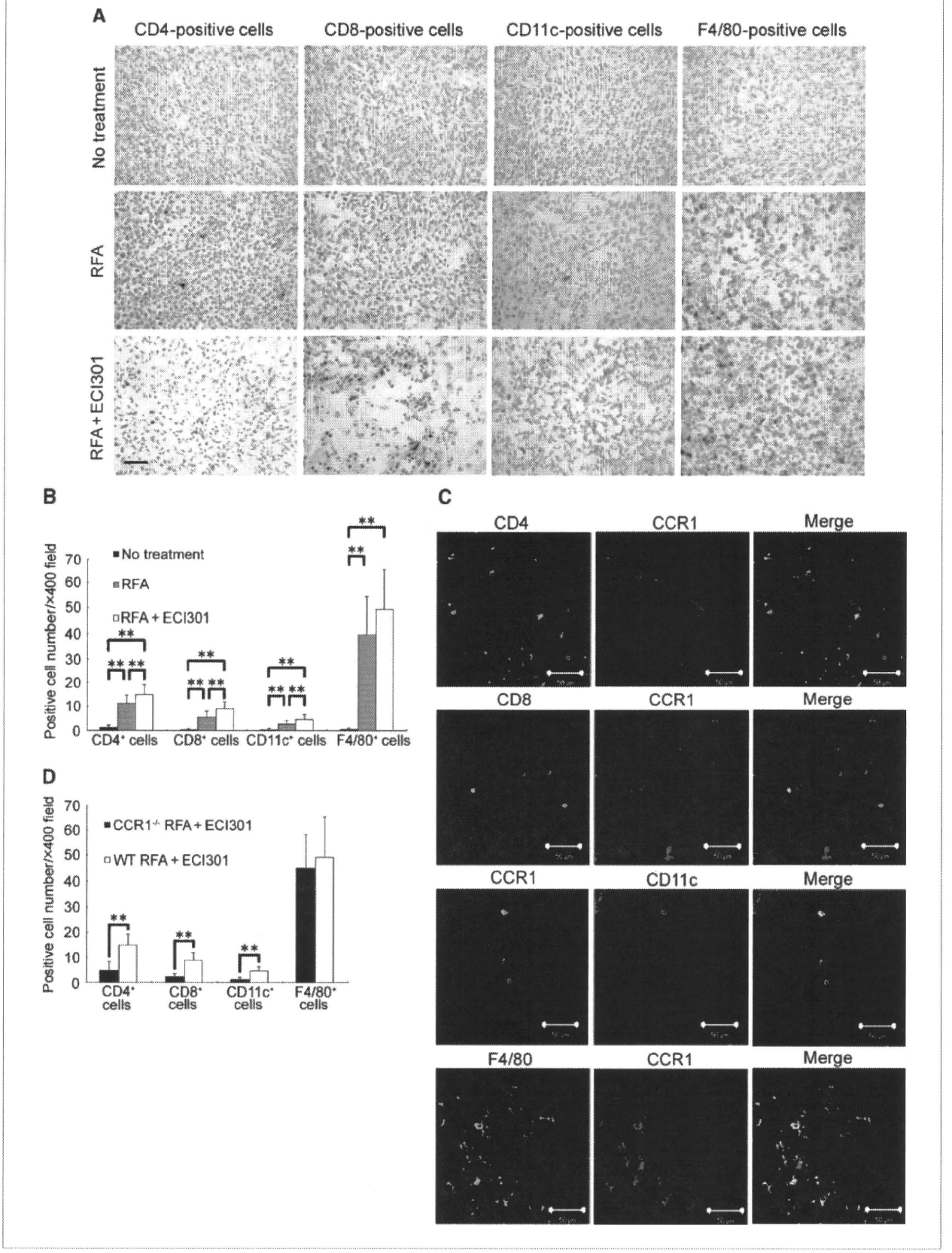

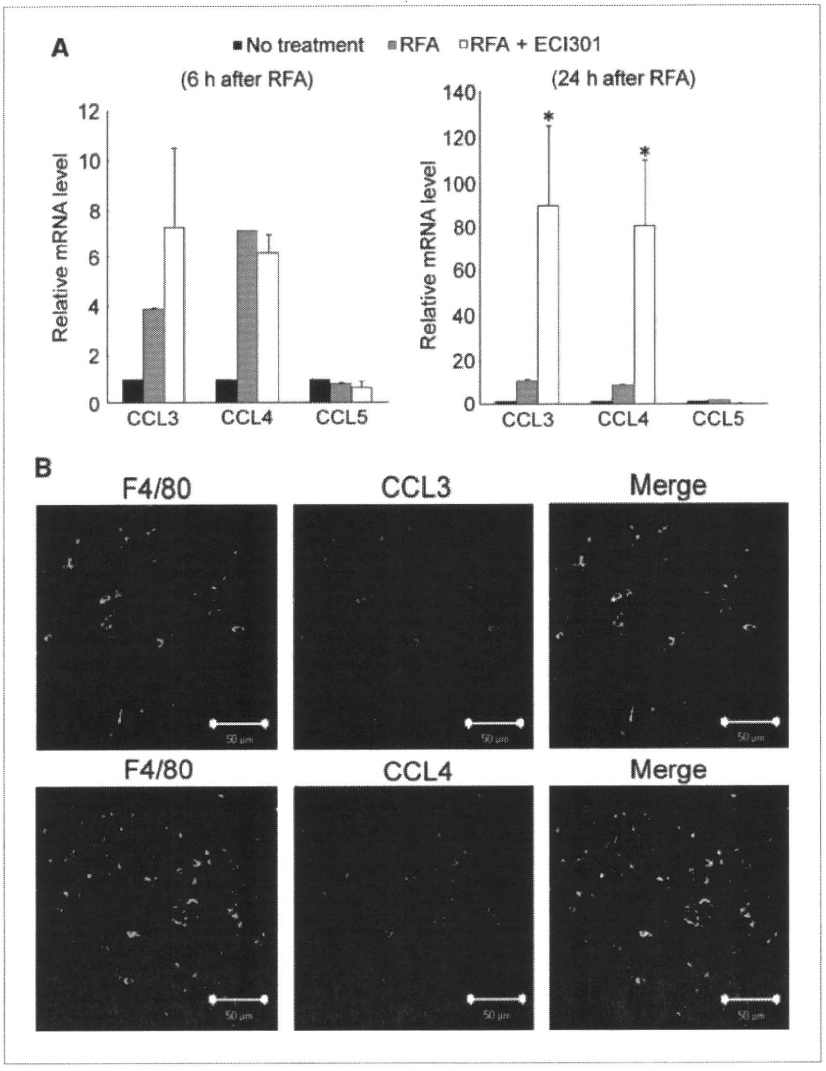

Figure 5. Increased CCL3 expression in RFA-treated tumors. A, real-time RT-PCR was performed on total RNA extracted from RFA-treated tumors of WT mice. The tumors were harvested 6 h (left) or 24 h (right) after RFA. Chemokine mRNA levels were normalized to GAPDH mRNA levels. Columns, mean ($n = 3$); bars, SD. *, $P < 0.05$, compared with untreated mice. B, RFA-treated tumors were removed from WT mice on day 1 after RFA plus ECI301 treatment and immunostained with the indicated combinations of antibodies as described in Materials and Methods. Right, digitally merged images. Representative results from three individual animals. Original magnification, ×400. Bar, 50 μm.

On the contrary, administration of ECI301 without RFA did not result in a significant decrease in tumor size (Fig. 1C). These observations suggest that ECI301 can augment RFA-induced antitumor effects but fails to induce antitumor effects by itself.

Deficiency of *CCR1* abrogates increased antitumor effect of ECI301 after RFA

ECI301 uses two distinct chemokine receptors, CCR1 and CCR5. To elucidate the roles of these chemokine receptors, either tumor-bearing *CCR1*$^{-/-}$ or *CCR5*$^{-/-}$ mice were similarly treated with RFA plus ECI301. RFA retarded the growth of non–RFA-treated tumors in *CCR1*$^{-/-}$ mice similar to that in WT mice, but ECI301 failed to further accentuate RFA-induced growth retardation of non–RFA-treated tumors (Fig. 2A). In contrast, ECI301 augmented RFA-mediated inhibition of non–RFA-treated tumors in *CCR5*$^{-/-}$ mice, resulting in complete tumor eradication in one of six mice (Fig. 2B). These observations indicate that CCR1-expressing, but not CCR5-expressing, cells play an important role in ECI301-induced augmentation of tumor regression after RFA.

ECI301 increases CCR1-expressing cells in peripheral blood and RFA-treated tumors after RFA

The reported capacity of CCL3 to mobilize leukocytes into peripheral blood (15, 16) prompted the investigation of the

Figure 4. ECI301 increases infiltration of CCR1-expressing leukocytes into RFA-treated tumors after RFA. RFA-treated tumors were removed from WT or *CCR1*$^{-/-}$ mice 8 h after RFA. A, B, and D, immunohistochemical analysis was performed using anti-CD4, anti-CD8a, anti-CD11c, or anti-F4/80 antibodies. A, representative results from three individual WT mice in each group. Original magnification, ×400. Bar, 50 μm. B and D, the numbers of CD4$^+$, or CD8$^+$, CD11c$^+$, or F4/80$^+$ cells were counted. Cell density was determined in 10 randomly chosen tumor areas at 400-fold magnification. Columns, mean ($n = 5$); bars, SD. **, $P < 0.01$. C, RFA-treated tumor tissues were processed using double-color immunofluorescence analysis as described in Materials and Methods. Right, digitally merged images. Representative results from three individual animals. Original magnification, ×400. Bar, 50 μm.

effects of ECI301 on peripheral blood. RFA alone had few effects on the numbers of CCR1-expressing cells, but subsequent ECI301 administration increased the numbers of CCR1-expressing cells in peripheral blood, particularly $CD11c^+$ cells, but not $CD4^+$ or $CD8^+$ cells (Fig. 3). Because immune cells need to accumulate in RFA-treated tumors at an early stage to initiate adaptive immune responses, CCR1 expression by tumor-infiltrating cells in RFA-treated tumors was examined 8 hours after treatment. RFA-induced $CD4^+$, $CD8^+$, $CD11c^+$, and $F4/80^+$ cell infiltrations into RFA-treated tumors were greater than those into tumors of untreated mice. Moreover, ECI301 further increased the numbers of $CD4^+$, $CD8^+$, and $CD11c^+$ cells infiltrating into RFA-treated tumors compared with the numbers of these cells infiltrating into tumors treated with RFA alone (Fig. 4A and B). In RFA-treated tumors, most $CD11c^+$ and $F4/80^+$ cells expressed CCR1, whereas few $CD4^+$ and $CD8^+$ cells expressed CCR1 (Fig. 4C). Furthermore, ECI301-induced $CD4^+$, $CD8^+$, and

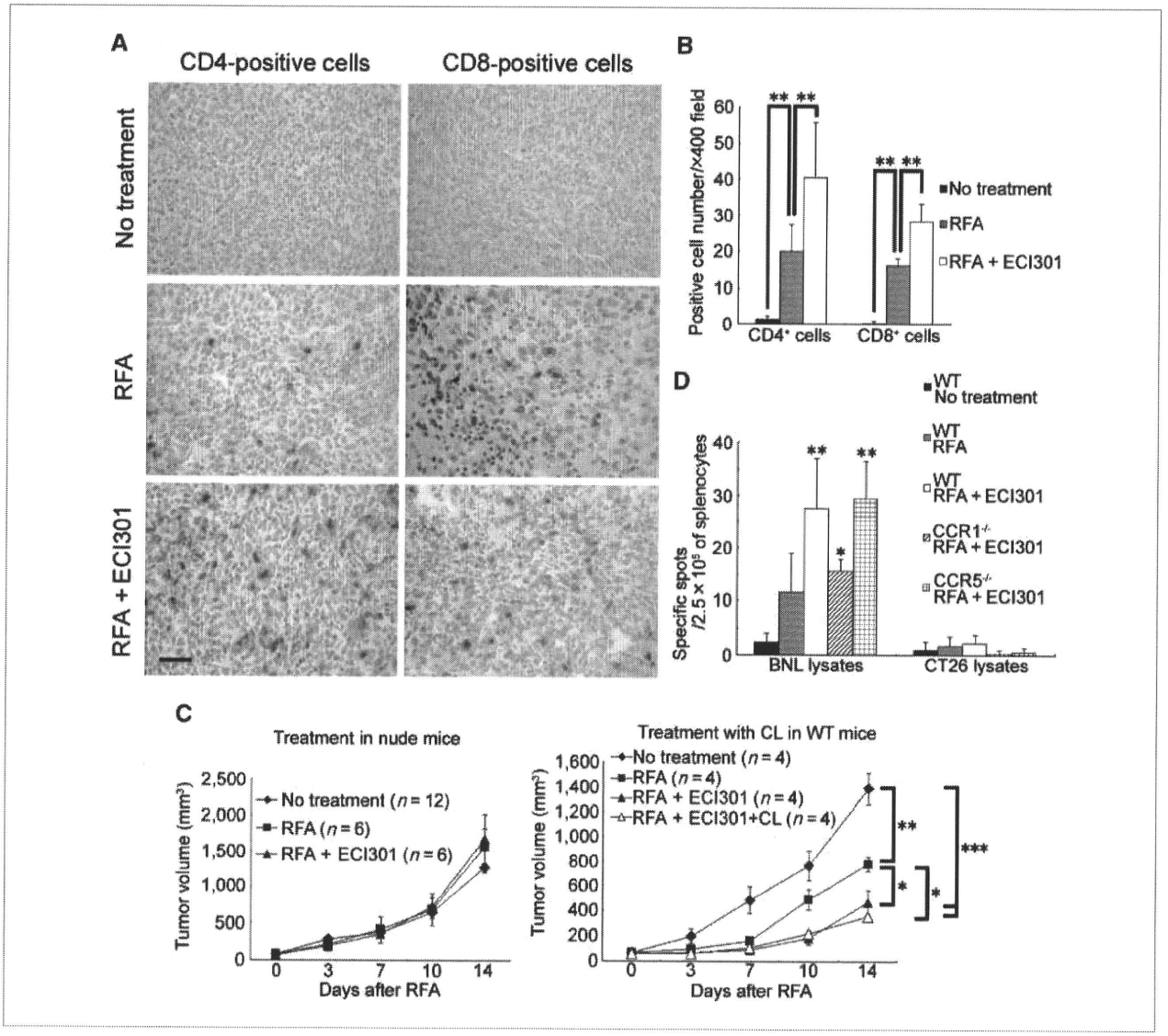

Figure 6. ECI301 augments tumor-specific immune responses after RFA. A, non–RFA-treated tumors were removed from WT mice on day 3 after RFA, and immunohistochemical analysis was done using anti-CD4 or anti-CD8a antibodies. Representative results from three individual animals in each group. Original magnification, ×400. Bar, 50 μm. B, the numbers of $CD4^+$ or $CD8^+$ cells were counted. Cell density was determined in 10 randomly chosen tumor areas at 400-fold magnification. Columns, mean (n = 5); bars, SE. **, $P < 0.01$. C, BALB/c-*nu/nu* mice (left) and BALB/c-WT mice (right) were inoculated with BNL cells and treated as described in the legend to Fig. 1. In the RFA + ECI301 + clodronate liposome (CL) group, the mice were injected with 200 μL of CL to deplete monocytes/macrophages as described in Materials and Methods. Non–RFA-treated tumor volumes were measured twice a week. Points, mean; bars, SE. D, spleens from WT, *CCR1*$^{-/-}$, or *CCR5*$^{-/-}$ mice were harvested on day 21 after RFA, and mononuclear cells were separated from the spleens for ELISPOT assay as described in Materials and Methods. The number of specific spots was determined by subtracting the number of spots in wells without lysates from the number of spots in wells with tumor lysates. Columns, mean (n = 3); bars, SE. *, $P < 0.05$; **, $P < 0.01$, compared with untreated WT mice.